![USGS logo - science for a changing world]

Water Availability and Use Science Program

Prepared in cooperation with the U.S. Fish and Wildlife Service and the National Fish and Wildlife Foundation

Sediment Mobility and River Corridor Assessment for a 140-Kilometer Segment of the Main-Stem Klamath River Below Iron Gate Dam, California

Open-File Report 2020–1141

U.S. Department of the Interior
U.S. Geological Survey

Sediment Mobility and River Corridor Assessment for a 140-Kilometer Segment of the Main-Stem Klamath River Below Iron Gate Dam, California

By Jennifer Curtis, Travis Poitras, Sandra Bond, and Kristin Byrd

Open-File Report 2020–1141

U.S. Department of the Interior
U.S. Geological Survey

U.S. Geological Survey, Reston, Virginia: 2021

Acknowledgments

Note: A mix of U.S. customary system of units and the International System of Units (SI) are used in this report. U.S. Geological Survey streamflow data and geospatial data were published using U.S. customary system of units, which also are used by the Klamath River flow management community.

Contents

Figures

Tables

Conversion Factors

U.S. customary units to International System of Units

Multiply	By	To obtain
Length		
foot (ft)	0.3048	meter (m)
mile (mi)	1.609	kilometer (km)
Flow rate		
cubic foot per second (ft³/s)	0.02832	cubic meter per second (m³/s)

International System of Units to U.S. customary units

Multiply	By	To obtain
Length		
millimeter (mm)	0.03937	inch (in.)
meter (m)	3.281	foot (ft)
kilometer (km)	0.6214	mile (mi)
kilometer (km)	0.5400	mile, nautical (nmi)
meter (m)	1.094	yard (yd)
Area		
square kilometer (km²)	247.1	acre
square kilometer (km²)	0.3861	square mile (mi²)
Volume		
liter (L)	33.81402	ounce, fluid (fl. oz)
liter (L)	2.113	pint (pt)
liter (L)	1.057	quart (qt)
liter (L)	0.2642	gallon (gal)
liter (L)	61.02	cubic inch (in³)

Multiply	By	To obtain
	Mass	
gram (g)	0.03527	ounce, avoirdupois (oz)
kilogram (kg)	2.205	pound avoirdupois (lb)

Datum

Vertical coordinate information for the stream gages is referenced to the National Geodetic Vertical Datum of 1929 (NGVD 29).

Vertical coordinate information for the geospatial data is referenced to the North American Vertical Datum of 1988 (NAVD 88).

Horizontal coordinate information is referenced to the North American Datum of 1983 (NAD 83).

Elevation, as used in this report, refers to distance above the vertical datum.

Abbreviations

ADCP   acoustic Doppler current profiler

DEM   digital elevation model

KCC   Klamath Community Center

PC   Portuguese Creek

REM   relative elevation model

RF   random forest

RKM   river kilometers

USFWS   U.S. Fish and Wildlife Service

USGS   U.S. Geological Survey

XML   extensible markup language

Sediment Mobility and River Corridor Assessment for a 140-Kilometer Segment of the Main-Stem Klamath River Below Iron Gate Dam, California

By Jennifer Curtis, Travis Poitras, Sandra Bond, and Kristin Byrd

Abstract

This river corridor assessment documents sediment mobility and river response to flood disturbance along a 140-kilometer segment of the main-stem Klamath River below Iron Gate Dam, California. Field and remote sensing methods were used to assess fundamental indicators of active sediment transport and river response to a combination of natural runoff events and reservoir releases during the study period from 2005 to 2019. Discharge measurements at two gaged sites and bed-material samples at two ungaged sites provided direct and indirect evidence of mobile bed conditions, scour and fill, and surface flushing of fine sediment. Available remote-sensing datasets collected in 2005, 2009, 2010, and 2016 were used to determine sediment storage, flood inundation boundaries, and provide indirect evidence of flood-induced scour. These datasets validate channel-maintenance flows defined by Shea and others (2016). During the study period, flows greater than or equal to 6,030 cubic feet per second mobilized the substrate, caused localized scour, and flushed fine sediment from bar surfaces. Flows greater than or equal to 10,400 cubic feet per second stripped vegetation from bars and floodplains and produced deeper scour. Flood disturbance within the study reach is produced by the combined effect of natural flows and reservoir releases, which resulted in mobile bed conditions during the study period. Periodic scour and substrate disturbance are considered by the U.S. Fish and Wildlife Service to be integral for managing disease-induced mortality of juvenile and adult salmonids. Substrate conditions conducive to parasites that host infectious diseases, particularly Ceratonova shasta, occur periodically. Additional studies are required to determine whether disease prevalence can be mitigated by well-timed reservoir releases. Study results are useful for interpreting linkages among physical and biological processes and for evaluating the effectiveness of flow management targeted to improve river bed conditions for endangered salmonid populations.

Introduction

The Klamath River (40,790 square kilometers [km²], fig. 1) is the third largest river in the continental United States flowing into the Pacific Ocean. The headwaters emerge from the Cascade Range in the high deserts of southeastern Oregon, and the river flows through northern California to its estuary located in the temperate coastal forests. A series of hydroelectric facilities (JC Boyle, Copco No. 1, Copco No. 2, and Iron Gate), owned and operated by PacifiCorp (Portland, Oregon), separate the river into upper and lower basins. The dams associated with the hydroelectric facilities block volitional fish passage and access to 420 miles of cold-water habitat in the upper basin (Department of the Interior and others, 2012). The presence of the dams and operation of the reservoir impoundments altered the flow and sediment transport regimes in the lower basin (Ayres and Associates, 1999; Holmquist-Johnson and Milhous, 2010; Department of the Interior and others, 2012; Shea and others, 2016).

In the upper basin, the Bureau of Reclamation (Reclamation) operates the Klamath Irrigation Project, which delivers water to irrigation districts in Oregon and California. Cumulative downstream impacts resulted in fisheries population declines that range from 52 to 95 percent for endangered coho salmon, greater than 90 percent for fall-run Chinook salmon, 98 percent for spring-run Chinook salmon, 67 percent for steelhead, and 98 percent for Pacific lamprey (National Research Council, 2004; Department of the Interior and others, 2012).
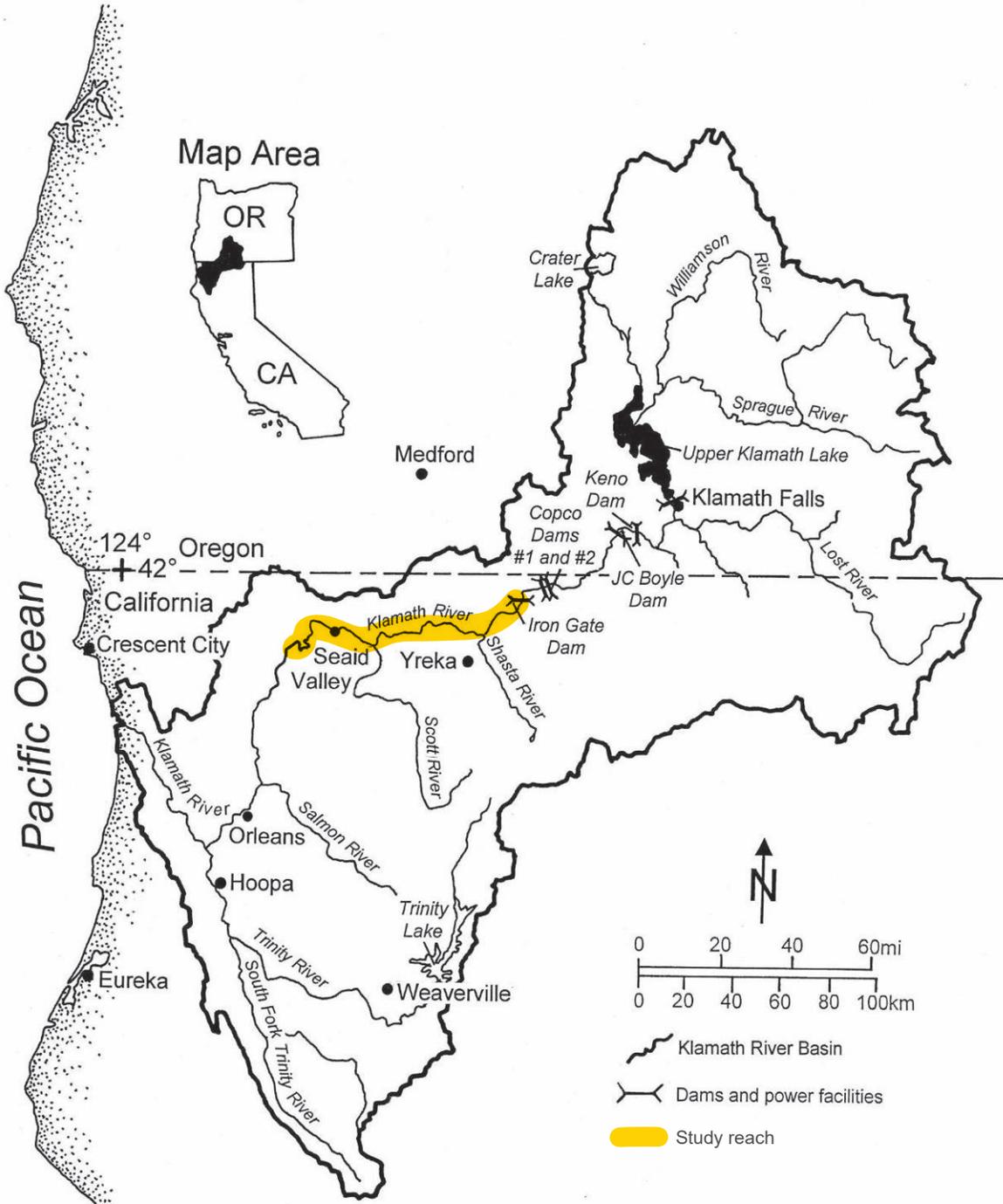
Figure 1.   Location of Klamath River Basin, study reach, principle streams, dams, and hydroelectric facilities, California and Oregon. Figure modified from Holmquist-Johnson and Milhous (2010).

The biological opinion (BiOp; National Marine Fisheries Service and U.S. Fish and Wildlife Service, 2013) described the effects of the Klamath Irrigation Project on water availability and critical habitat for federally listed salmonid species and determined minimum flow requirements. The 2013 BiOp also provided a summary of studies (Bartholomew and others, 1997; Stocking and Bartholomew, 2007) that identified *Manayunkia speciosa,* a freshwater polychaete, as the obligate invertebrate host for *Ceratonova shasta* (syn *Ceratomyxa shasta*), a myxosporean parasite, known to cause substantial mortality in juvenile and adult salmonids.

Recent studies (Malakauskas and others, 2013; Wright and others, 2014; Alexander and others, 2016) indicated that the spatial distribution and abundance of the polychaete host decreases when their preferred habitat is disturbed during high-flow events that scour or mobilize the channel substrate. This assertion suggests that surface-flushing, deep-flushing, and armor-disturbing flow events, collectively referred to herein as channel-maintenance flows, could be useful for reducing polychaete abundance, fish disease prevalence, and disease-induced mortality of juvenile and adult salmonids caused by *C. shasta*.

Channel-maintenance flows produce hydrologic disturbance, an essential process that maintains ecological function in rivers (Poff and others, 1997; Puckridge and others, 1998; Whiting, 2002; Arthington and others, 2006). In this study, hydrologic disturbance is synonymous with flood disturbance (Bendix, 1997; Schmidt and Potyondy, 2004) that scours and disturbs the substrate; mechanically strips and uproots aquatic and riparian vegetation; and dislodges polychaetes adhered to the substrate.

Channel-maintenance flows are broadly classified into two categories (Kondolf and Wilcock, 1996). "Flushing flows" modify the textural composition of the channel substrate by removing surficial and interstitial fine sediment. "Channel forming" flows mobilize coarser material to maintain channel form and produce overbank flows that augment flow and

sediment to floodplains to maintain connectivity. In regulated rivers, channel-maintenance flows are a useful management tool for initiating bed mobility, substrate disturbance, and active sediment transport (Wilcock and others, 1996).

This study, completed in cooperation with the U.S. Fish and Wildlife Service Arcata Field Office and the National Fish and Wildlife Foundation, builds upon a substantial amount of previous work (Ayres and Associates, 1999; Hardy and Addley, 2001; Holmquist-Johnson and Milhous, 2010; Bureau of Reclamation, 2011). Collectively, these previous studies summarized the history of anthropogenic impacts, discussed the importance of large flows for reworking channel substrates, and proposed channel-maintenance flows necessary to achieve a range of substrate movement states along the main-stem Klamath River below Iron Gate Dam. In addition, Foott and others (2011) developed a conceptual model to explain the linkages among flow history, scour events, polychaete abundance, and fish disease (fig. 2). The science (National Marine Fisheries Service and U.S. Fish and Wildlife Service, 2013) that supports this conceptual model was used to develop recommendations for channel-maintenance flow thresholds and substrate movement states (table 1; Shea and others, 2016) to decrease *C. shasta* infection rates and improve juvenile rearing habitat downstream from Iron Gate Dam (fig. 1).
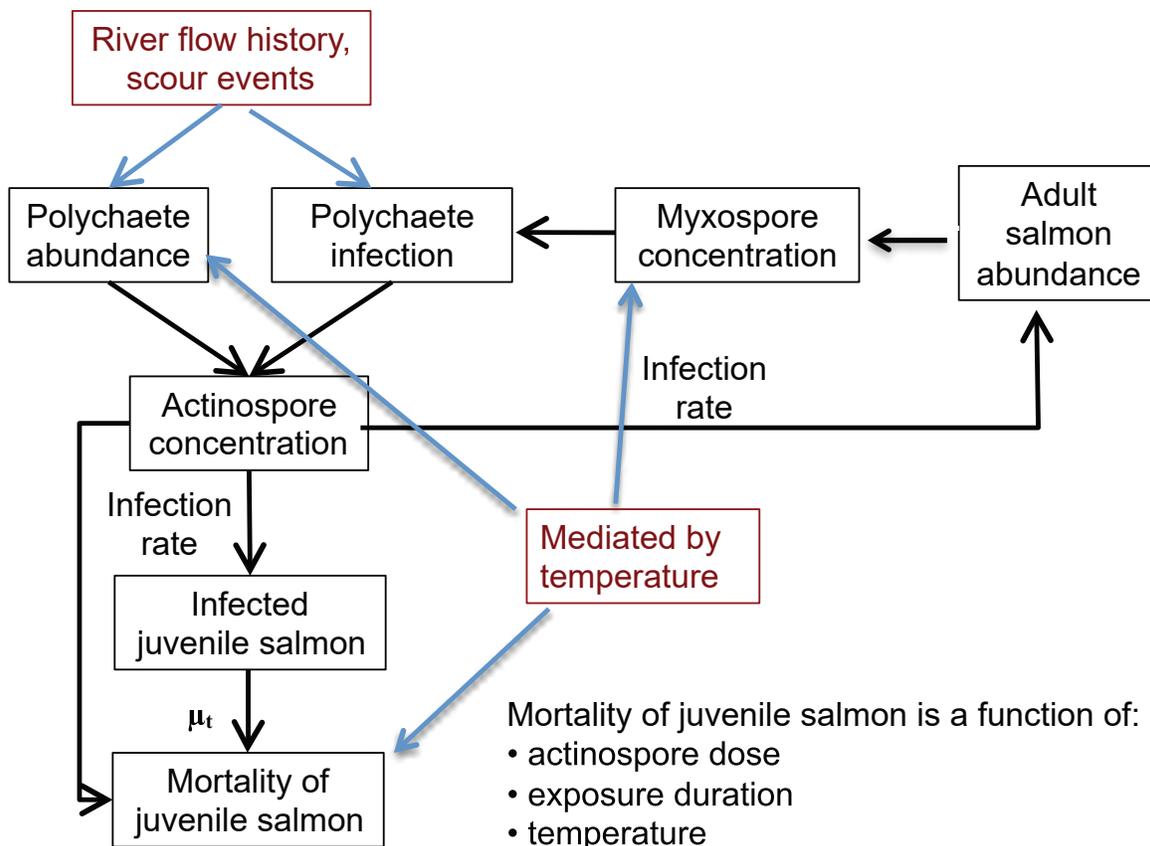
Figure 2.   Conceptual model for variables that influence infection caused by *C. shasta* and mortality of juvenile Chinook salmon. **Abbreviation**: µt is the mortality rate of infected juvenile salmon estimated from weekly actinospore concentration, Foott and others, 2011.

Table 1.   Substrate movement states and flow thresholds defined for the main-stem Klamath River below Iron Gate Dam (Shea and others, 2016).

[From Shea and others (2016). **Abbreviations**: ft³/s, cubic foot per second; <, less than; %, percent; >, greater than]

Substrate movement state	Description	Streamflow (ft³/s)
Immobile bed	No movement of surface sediment, armor layer or substrate. Deposition of suspended sediment absorbed into voids (until full).	<2,500
Stable bed	No movement of surface sediment, armor layer or substrate. Suspended sediment in water column remains in transport.	<5,000
Surface flushing	Movement of surface fines on 20–30% of bed.	<8,700
Deep flushing	Removal of in-filled fine sediment from armor layer.	<11,250
Armor disturbance	Movement of individual armor layer particles.	<15,000
Armor layer movement	Reworking of armor and substrate layers.	>15,000

In the lower Klamath River, a primary goal of channel-maintenance flows is management of disease-induced mortality of juvenile and adult salmonids (Shea and others, 2016; Som and Hetrick, 2016; Som and others, 2016a, b). Flow objectives related to disease management include flushing of fine sediment; mobilization and scour of coarser substrate material; disturbance of preferred polychaete habitat; and disruption of the life cycle of *C. shasta*. An additional objective is deterrence of vegetation encroachment, which stabilizes the edge of the low-flow channel and may result in channel narrowing and loss of low-velocity rearing habitat for juvenile salmonids.

Shea and others (2016) used sediment entrainment analyses from three independent studies (Ayres and Associates, 1999; Holmquist-Johnson and Milhous, 2010; Bureau of Reclamation, 2011) to define a range of flows necessary to achieve several channel substrate movement states (fig. 3). These entrainment studies used uncalibrated sediment transport equations to estimate the critical discharges required to initiate various stages of sediment mobilization. Beginning in 2017, implementation of the channel-maintenance flows defined by Shea and others (2016) was mandated by a U.S. District Court Order Injunction (Case No. 3:16-cv-04294-WHO, Northern District of California March 24, 2017).

Objectives

The U.S. Fish and Wildlife Service (USFWS) Arcata Field Office requested an assessment of sediment mobility and river corridor conditions for the primary salmonid spawning reach along the main-stem Klamath River below Iron Gate Dam, California (figs. 1, 3). Disturbance of the river substrate is considered by the USFWS to be integral for managing disease-induced mortality of salmonids in the spawning reach below Iron Gate Dam (Foott and others, 2011; Shea and others, 2016). Specific study objectives were to (1) relate sediment mobility to flow history, (2) validate channel-maintenance flows defined by Shea and others (2016), (3) assess river corridor conditions conducive to *C. shasta*, and (4) evaluate the effectiveness of flow management targeted to improve river conditions for endangered salmonid populations.

Purpose and Scope

In this report, a combination of field and remote sensing methods was used to assess sediment mobility and river response to flood disturbance. Flood disturbance from 2005 to 2019 is examined along with river corridor conditions. Fundamental indicators of active sediment transport are used to provide direct and indirect evidence of sediment mobility, before and after implementation of court-mandated channel-maintenance flows in 2017. This report assesses mobile-bed conditions, flushing of surface fines, sediment storage, and flood-induced scour of bars and floodplains. Study results are related to channel-maintenance flow targets defined by Shea and others (2016). The scope of the report is limited to physical habitat and riparian vegetation conditions during the study period; quantitative relations to fish health or pathogens were not measured.
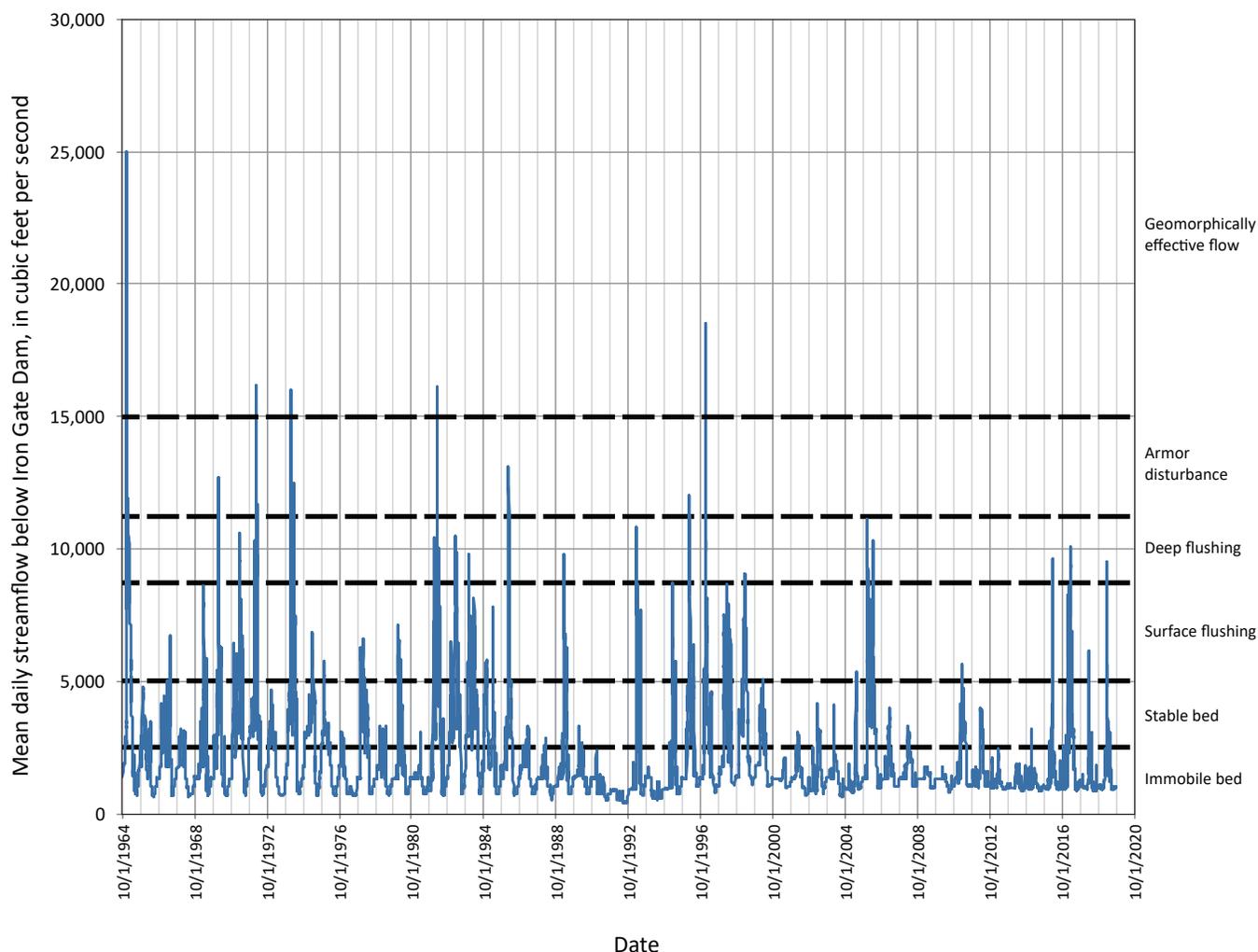
Figure 3.   Mean daily streamflow of the Klamath River below Iron Gate Dam for water years 1965–2019 with substrate mobilization states defined by Shea and others (2016). Data available at https://waterdata.usgs.gov/nwis.

Study Area

The 140-kilometer (km) study reach begins immediately below Iron Gate Dam and extends to 2 km below the Indian Creek confluence (fig. 4). Within the study reach, the location of reach-scale sediment storage in bars and floodplains generally is fixed in space, and channel position is constrained by rock outcrops, terraces, tributary fans, and landslides. Local channel dimensions vary with confinement. Floodplains are poorly developed, discontinuous, and formed dominantly by vertical sediment accretion through overbank deposition, rather than lateral accretion through channel migration and point-bar deposition. Extensive sections of the study reach are morphologically stable with dense stands of woody and herbaceous riparian vegetation along the low-flow, wetted-channel edge.

Streamflow in the upper basin, above Iron Gate Dam, is produced primarily from groundwater and snowmelt discharge and is heavily regulated by flow management associated with the Reclamation's Klamath Irrigation Project (National Research Council, 2004; National Marine Fisheries Service and U.S. Fish and Wildlife Service, 2013). In the lower basin, below Iron Gate Dam, streamflow is produced primarily by flows from the upper basin during the low-flow season and by rainfall-runoff during the remainder of the water year (Thorsteinson and others, 2011). The study reach (fig. 4) includes two U.S. Geological Survey (USGS) streamflow gaging stations (Klamath River below Iron Gate Dam CA, USGS 11516530 [IGD]; Klamath River near Seiad Valley CA, USGS 11520500 [SEIAD]; U.S. Geological Survey, 2020). Large interannual and intra-annual variations in streamflow are common and increase with distance downstream from Iron Gate Dam (fig. 5).

A.
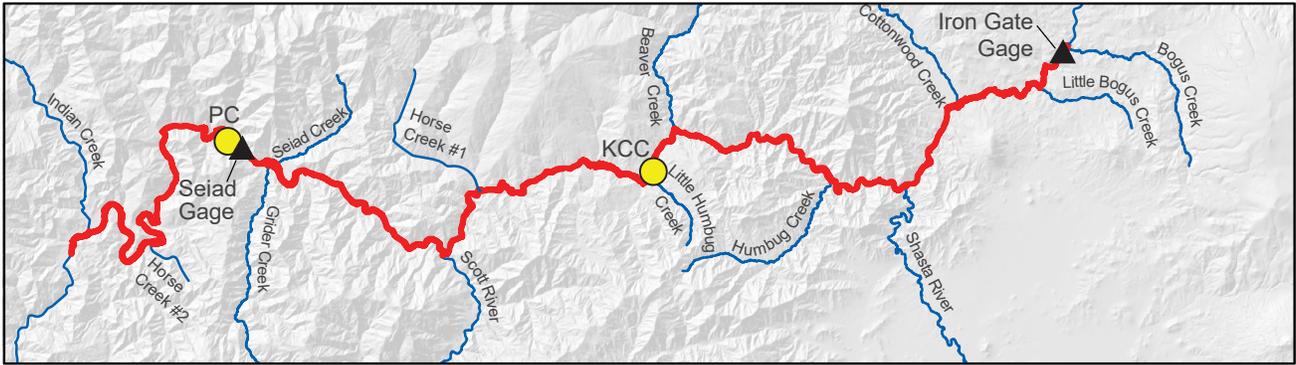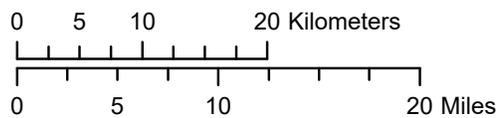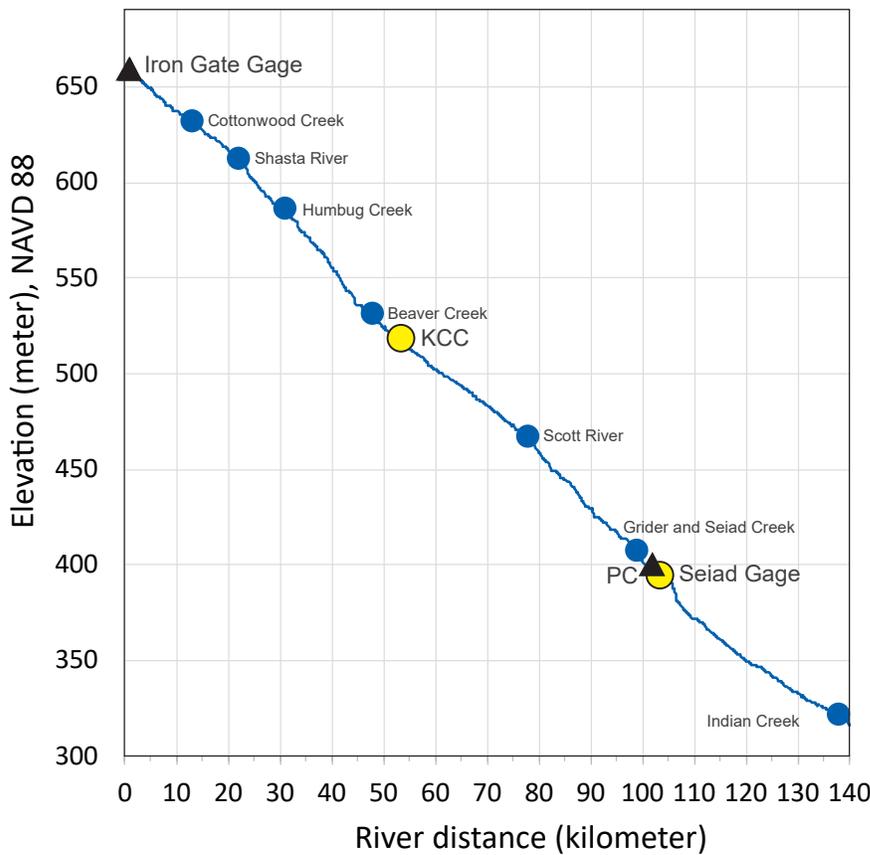
B.

Figure 4.   Depictions of the 140-kilometer study reach along the main-stem Klamath River below Iron Gate Dam, California, as *A*, shaded-relief map; and *B*, longitudinal profile of water surface elevation. Locations are shown for two gaged sites (Iron Gate Dam, USGS 11516530; Seiad Valley gage, USGS 11520500) and two sediment-sampling sites (Portuguese Creek, PC; Klamath Community Center, KCC).
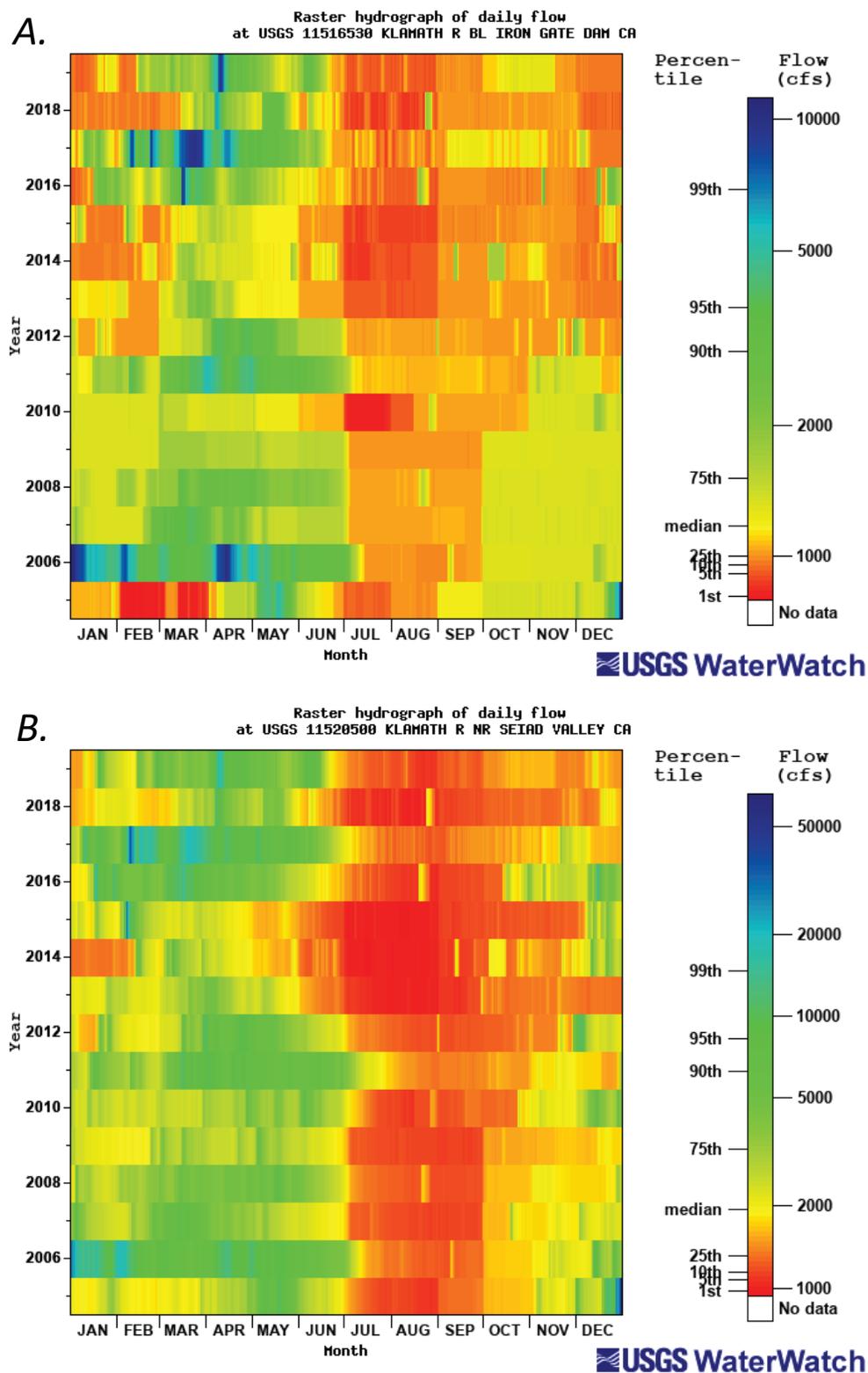
Figure 5.   Raster hydrographs for *A*, Klamath River below Iron Gate Dam (USGS 11516530); and *B*, Klamath River near Seiad Valley (USGS 11520500) for water years 2005–19. Water year is depicted on the vertical axis, months and days are depicted on the horizontal axis, and mean daily streamflow is depicted by the color. (Data available at https://waterdata.usgs.gov/nwis. See fig. 4 for gage location and table 2 for gage descriptions.)

Generally, fine-sediment transport occurs more frequently than coarse-sediment transport, and the frequency of transport events depends on the relation between sediment supply and transport capacity. For example, in supply limited reaches, fine sediment may be selectively transported over coarser material. This condition results in short residence times for fine-sediment storage and longer residence times for coarse-sediment storage. Ayres and Associates (1999) suggested that selective transport in the study reach resulted in equilibrium conditions over the long term with little change in coarse-sediment storage.

Methods

A combination of field and remote sensing methods was used to assess bed mobility and river corridor response to flood disturbance. At two gaged sites, discharge measurements were used to define sediment-mobilization thresholds and to infer episodic scour and fill from changes in mean bed elevations. At two ungaged sites, bulk samples of the bed substrate were used to assess the presence of fine sediment and the effectiveness of surface-flushing flows. A digital elevation model (DEM) and orthophotos collected in 2010 were used to quantify sediment storage and to define flood-inundation boundaries for flow events with 2-year, 5-year, and 10-year recurrence intervals. A time series of orthophotos from 2005, 2009, and 2016 was used to assess the response of riparian vegetation to the 2006 scour event, which was followed by a drier period that included the 2012–16 drought (Lund and others, 2018). These datasets, along with field observations following the 2017 peak flow, were used to relate sediment mobility to flow history and evaluate the effectiveness of channel-maintenance flows.

Sediment Mobility

Discharge Measurements at Two Study Gages

Monthly discharge measurements are routinely made at USGS stream gages using a variety of methods (Turnipseed and Sauer, 2010). These measurements are publicly available (U.S. Geological Survey, 2020). Since 2016, acoustic Doppler current profilers (ADCPs) with bottom tracking were used to make cross-sectional moving-boat discharge measurements at the two study gages.

Standard USGS protocol requires a moving-bed test for ADCP discharge measurements (Mueller, 2016) that use bottom tracking to determine the boat velocity relative to the bed. Water velocity is measured relative to the ADCP, and if the boat velocity is known, the apparent velocity of the bed can be determined (Rennie and others, 2017). If the ADCP is mounted on a moving boat, corrections are made to obtain an accurate water velocity measurement. This is necessary because sediment transport, on or near the streambed, causes

a Doppler shift in the bottom-tracking ping resulting in boat-velocity measurements that are biased in the upstream direction. This phenomenon is commonly referred to as a "moving bed."

The ratio of bed velocity to flow velocity, expressed as a percent and referred to as the percent moving bed (Mueller, 2016), is recorded for each ADCP measurement. If 1 percent or more of the bottom tracks indicate a moving bed, the discharge measurement is flagged with a warning that states a moving bed is present and the ADCP measurement requires a correction. Although the moving-bed test provides evidence of sediment transport on or near the bed, this test cannot be used to determine whether mobile material was entrained locally or was transported downstream from entrainment upstream and then passed the measurement cross section over an otherwise stable bed.

The metadata for each discharge measurement is recorded in an extensible markup language (XML) file. Various statistics and characteristics of the measurement recorded in the XML files are used to assess the quality of the measurement. The XML files include an accuracy rating that is based on the hydrologic and hydraulic conditions during the measurement. For example, measurements are rated excellent (accuracy plus or minus 2 percent), good (plus or minus 5 percent), fair (plus or minus 8 percent), or poor (more than 8 percent). The estimated boat and bed velocities and results from the moving-bed test are also are recorded in the XML file.

Discharge measurements, with accuracies of fair (plus or minus 8 percent) or better, were plotted against the percent moving bed estimates. Sediment-mobilization thresholds for the two study gages were then defined using the minimum discharge associated with a percent moving bed of greater than or equal to 1 percent. This minimum discharge can be used as a proxy for incipient motion.

The data used in the moving-bed analysis, which includes the corrected discharge, gage height, and flow velocities published on-line in the USGS National Water Information System (NWIS, U.S. Geological Survey, 2020), along with the ADCP estimates of bed velocity and flow velocity and the derived percent moving bed, are available within the XML files associated with each discharge measurement (tables 1.1, 1.2). The XML files for each discharge measurement are available at https://doi.org/10.3133/ofr20201141.

Changes in mean bed elevations from 2005 to 2019 were estimated from routine discharge measurements (Smelser and Schmidt, 1998; Juracek and Fitzpatrick, 2009), which were made at cross-section locations pre-determined for each of the study gages. At each of the study gages, non-wading measurements were made routinely from an anchored cableway.

Changes in mean bed elevation were estimated for flows less than or equal to the mean annual flow (table 2). The study gages are within confined reaches with steep channel banks where increases in discharge are accompanied by small increases in width but large increases in water depths.

Table 2.   Description of two U.S. Geological Survey (USGS) stream gages, mean discharge, and discharges for high flows with recurrence intervals of 2 years (Q2), 5 years (Q5), 10 years (Q10), and 25 years (Q25) as estimated by the Bureau of Reclamation, 2011.

[See figure 4 for gage locations. **Abbreviations**: ID, identification; km², square kilometers; ft³/s, cubic foot per second; IGD, Iron Gate Dam gage; SEIAD, Seiad Valley gage]

USGS station number	USGS station name	Station ID	Drainage area (km²)	Mean annual flow (ft³/s)	Q2 (ft³/s)	Q5 (ft³/s)	Q10 (ft³/s)	Q25 (ft³/s)
11516530	Klamath River below Iron Gate Dam CA	IGD	4,630	1,945	6,030	10,980	15,610	21,460
11520500	Klamath River near Seiad Valley CA	SEIAD	6,940	3,705	17,600	39,960	56,540	93,100

The mean annual flow was used as a reference discharge to minimize the influence of variations in channel widths on the flow depths used to estimate bed elevations.

Cableway measurements for flows less than or equal to the mean annual flow were used to estimate mean bed elevations using the continuity equation:

$$Q = A \times v \qquad (1)$$

where

	Q	is discharge,
	A	is cross-sectional area, and
	v	is velocity.

Mean water depth was calculated using:

$$\text{Mean depth} = Q/(w \times v) \qquad (2)$$

where

	w	is channel width.

The mean bed elevation, relative to the contemporary local gage datum, was then calculated using:

$$\text{Mean bed elevation} = \text{gage height} - \text{mean depth} \qquad (3)$$

Episodic scour and fill were inferred from the changes in mean bed elevation. A decline in bed elevation was interpreted as scour and an increase in bed elevation was interpreted as fill. The equations listed above can be used with U.S. customary units or the International System of Units (SI) as long as a single system of units is used consistently.

Bed-material Samples at Two Ungaged Sites

In September of 2018, bed-material samples were collected at two ungaged sites (fig. 4) previously sampled by Holmquist-Johnson and Milhous (2010). Klamath Community Center (KCC) is located 53-km downstream and Portuguese Creek (PC) is located 103-km downstream from Iron Gate Dam. Hereafter, we refer to river kilometers downstream from Iron Gate Dam using the abbreviation RKM. At each site, bulk sediment samples of recently mobilized bed material were collected at the apex of low elevation bars near the upstream riffle. Recently mobilized bed-material was identified as loose deposits of clean clasts without biofilms or staining (Wilcock and others, 2009).

A total of six bed-material samples, including four surface samples and two subsurface samples, were collected at each site using standard methods (Bunte and Abt, 2001). Four sample plots were randomly selected by blindly tossing a 0.5-meter (m) quadrat. To test the influence of vegetation on substrate grain size, two vegetated and two unvegetated plots were selected. At each site, surface samples were collected from all four plots and one vegetated and one unvegetated plot was selected for subsurface sampling. Surface samples were collected to a depth equal to the maximum clast diameter exposed within the plot. Subsurface samples were collected to a depth equal to the maximum clast diameter exposed on the bar surface.

Samples were hand shoveled into 20-liter (L) buckets and field sieved from 256 millimeters (mm) down to 8 mm in 0.5-phi grain size classes, where 1.0 phi is equal to $-\log_2$ multiplied by grain size in millimeters. Clasts greater than 64 mm were hand-sieved into classes using a gravelometer. Clasts between 64 mm and 8 mm were separated into classes using a rocker-sieve. The field-dried weight of the material within each grain size class was determined to the nearest 0.25 kilogram. The remainder of the sample, which contained clasts less than 8 mm, was sent to the USGS California Water Science Center Santa Cruz Sediment Lab where a 250-gram (g) subsample was created using an aluminum vane splitter. The subsample was sieved at 1-phi intervals from 8 mm down to 0.063 mm. The lab weights of material within each grain size class were determined to the nearest 0.1 g and subsample weights were adjusted by total sample weight. The field weights and lab weights were combined and used to determine the grain size distribution for the entire bulk sample.

Riparian Corridor Assessment

Geomorphic Features and Sediment Storage

A thematic map of geomorphic features was created in an ArcGIS (v.10.6) geodatabase using an available 2010 DEM and associated orthophoto (table 3; Woolpert, Inc., 2010). A mapping protocol was designed to assess ecologically important channel and riparian features relevant to fisheries management. The mapping protocol was hierarchical and similar to recent mapping on the Trinity River (Curtis and Guerrero, 2015; Curtis and others, 2015), the largest tributary to the Klamath River. Geomorphic features include uplands, floodplains, channel margins, high bar, low bar, secondary water features (ponds, split-flow channels, side channels, alcoves), rock outcrops, and the primary wetted channel (table 4).

The geodatabase includes a polygon feature class constructed using fields and domains with coded values (table 5), which enabled dynamic selection of attributes for channel and riparian features. A detrended DEM, or relative elevation model (REM), was used as the base map. Channel features were assigned to either main-stem or tributary environments. At tributary confluences, main-stem and tributary features were distinguished by the general trajectory of the feature. The main-stem and tributary channel trajectories were typically orthogonal to one another. Main-stem features were parallel to the main-stem channel trajectory, and tributary features were parallel to tributary channel trajectories. The minimum size for a mappable feature was 30 square meters. Linework for all the features within the geodatabase was reviewed at a scale of 1:2,000 to ensure consistency between study reaches.

The REM was created by removing the water-surface trend from the 2010 DEM. A channel centerline was manually digitized, and water surface elevations were extracted from the DEM and assigned to continuous points created along the centerline. A trend raster was created by extrapolating the water surface elevations for each point to the study area boundary using inverse-distance weighting. The REM was created by subtracting water surface elevations in the trend raster from the topographic elevations in the DEM. The resulting REM is a raster grid file with values assigned to each pixel that represent relative elevations above the local water surface.

During a field reconnaissance in October 2017, field observations of scour and mobility were collected at 30 sites distributed throughout the study reach following the 2017 deep-flushing flows (fig. 3). At each site, indicators of active sediment transport were assessed and recorded (embeddedness, surface fines, subsurface fines, loose bed, imbrication of coarse clasts, and presence of bedforms). In this study, fine sediment includes sand and finer particles (less than 2 mm in diameter).

The 140-km study area was split at RKM 71 into upstream and downstream segments of equal longitudinal distance. Separate mapping schemas were defined for the upstream and downstream segments (table 6) on the basis of the 2017 field observations of scour and mobility and to consider increases in stage with increasing distance downstream. The mapping schema provided a hierarchical mapping framework along a continuous elevational gradient.

The upstream and downstream schema were used to create two classified REM rasters, which were used to delineate channel and riparian features on the basis of their relative elevations above the local water surface. The two classified REMs were exported to polygon files, with each polygon representing a separate geomorphic feature. The polygons were imported into the geodatabase and attributes were assigned manually. The geodatabase and the associated metadata explaining the geospatial processing steps were published separately (Curtis and Bond, 2020). Herein, we explain the mapping protocol and criteria and provide detailed descriptions of the channel and riparian features.

Table 3. Description of geospatial datasets used to spatially assess the geomorphology and riparian vegetation of the main-stem Klamath River corridor, California.

[m, meter; ft3/s, cubic foot per second; ft, foot; NAIP, National Agriculture Imagery Program; m2, square meter]

Geospatial data sources	Acquisition date	Raster resolution (m)	Discharge at Iron Gate Dam (ft3/s)	Gage height Iron Gate Dam (ft)	Discharge at Seiad Valley (ft3/s)	Gage height Seiad Valley (ft)
NAIP orthophoto 3-band, Leaf-on	Aug. 18–21, 2005	1.0	976–987	2.40–2.46	1,070–1,090	2.40–2.46
NAIP orthophoto 4-band, Leaf-on	June 22–23, 2009	1.0	1,510	3.05–3.10	1,960–2,000	3.15–3.27
Orthophoto 3-band, Leaf-off	Mar. 18–19, 2010	0.3	1,420–1,470	2.85–3.01	2,470	3.75–3.79
LiDAR 8 pts / m2	Feb. 27–Mar. 15, 2010	0.3	1,330–1,740	2.79–3.39	2,270–2,890	3.67–4.21
NAIP orthophoto 4-band, Leaf-on	June 13–20, July 6, Aug. 7–13, 2016	0.6	915–1,110	2.03–2.51	1,070–2,020	1.99–3.31

Table 4. Definitions for geomorphic features within the river corridor along a 140-kilometer segment of the main-stem Klamath River, California.

[See companion data release (Curtis and Bond, 2020) for additional details. **Abbreviations**: ft, feet; RKM, river kilometer; >, greater than; ≤, less than or equal to; m, meter]

	Feature description
	Terrestrial features
Uplands	Uplands include undifferentiated areas underlain by soil, colluvium, alluvium, bedrock or legacy mine tailings. Defined using relative elevation classes: 15-ft upstream from RKM 71 and 20-ft downstream from RKM 71. Inundated by flows with recurrence interval of >10 years.
Floodplains	Discontinuous alluvial feature adjacent to the active channel and typically exhibits a vegetation gradient with the highest density of vegetation along the active-channel margin; density decreases with increasing distance from the channel margin. Defined using relative elevation classes: 10-ft upstream from RKM 71 and 13-ft downstream from RKM 71. Inundated by flows with recurrence interval of 10 years.
Ponds	Aquatic features disconnected from the active-channel boundary. Only areas containing water in the base imagery were mapped, even when it was apparent that additional areas would be inundated seasonally.
Other	Unique features with details of interest included in the 'Notes' field.
	Channel features
Wetted channel	Primary channel that delivers the majority of flow and where the channel splits, it is identified as the widest channel. Delineated by the wetted perimeter as seen in the 2010 base imagery.
Secondary water features	Wetted-channel features that do not deliver the majority of channel flow. Only areas containing water in the 2010 base imagery were mapped, even when it was apparent that additional areas were inundated at higher flows.
Alcove	Secondary water feature connected at one end to another wetted-channel feature (mainstem, tributary, side-channel, or split-flow channel).
Pond	Secondary water feature disconnected from any other wetted-channel feature.
Side channel	Narrow secondary channels connected to the primary channel at the upstream and downstream ends and distinguished from split-flow channels by conveyance of less than 20 percent of total summer base flow and generally less than 10 percent. The percentage of flow conveyance was estimated using channel width.
Split-flow channel	Secondary channels created by flow separation that results in a change in the river morphology. Split-flow channels convey between 20 and 50 percent of base flow. The percentage of flow conveyance was estimated using channel width.
Bar	Alluvial feature created and maintained by bedload transport typically oriented parallel to the primary flow direction. The boundary between bars and adjacent riparian or upland features may be gradual. Boundary was delineated using relative elevations, observational criteria that included morphology, vegetation type and density, and physical evidence of scour or deposition. Manually edited and field checked for evidence of active bedload transport (imbrication, bedforms, loose bed material).
Channel margin	Catch-all category for steep margins that exist between floodplain and wetted channel, where the relative elevation model delineates a transition between two or more relative elevation classes within a narrow horizontal distance (≤15 m). This features class may extend longitudinally more than one meander length and may include two or more undifferentiated features (for example, low bar, high bar, and rock outcrop).
Rock outcrop	Non-alluvial feature that is typically darker colored than alluvial features and may have a rough tone, jagged boundary, and may show lineations indicative of bedrock texture.
Other	Unique features with details of interest included in the 'Notes' field.
	Bar classification
Lateral	Depositional feature created and maintained by active bedload transport and attached to the channel margin.
Medial	Depositional feature created and maintained by active bedload transport and surrounded by water on all sides.
Low	Defined using relative elevation classes: 4-ft upstream from RKM 71 and 4-ft downstream from RKM 71. Inundated by flows with recurrence interval of 2 years.
High	Defined using relative elevation classes: 6-ft upstream from RKM 71 and 8-ft downstream from RKM 71. Inundated by flows with recurrence interval of 5 years.

Table 5.   Subtypes, domains, and coded values used as feature attributes for a database of geomorphic features along a 140-kilometer segment of the main-stem Klamath River, California.

[See companion data release (Curtis and Bond, 2020) for additional details. **Abbreviation**: =, equal to]

CODED VALUE	
Subtype field = environment type	
1	Main channel
2	Tributary
3	Terrestrial
Domain = terrestrial features	
6	Uplands
2	Floodplain
5	Secondary water feature
1	Other
Domain = channel features	
1	Wetted channel
2	Secondary water features
3	Bedrock
4	Bar
5	Other
6	Channel margin
Domain = secondary water features	
1	Alcove
2	Pond
3	Side channel
4	Split-flow channel
Domain = bar type	
1	Lateral
2	Medial
Domain = bar elevation class	
1	High
2	Low

The geodatabase includes a single vector file composed of polygon features with attributes assigned to each feature. Elevation differences between uplands and floodplains were distinct and these polygons did not require editing. The elevation gradient between the wetted channel edge, low bars, and high bars was gradual, and these features were manually edited by cross-checking polygon boundaries with field observations and interpretation of the 2010 orthophoto. Steep channel margins with a mix of alluvial and non-alluvial features presented a unique case and these features were lumped into a single feature class simply called "channel margin." The edge of the wetted channel and rock outcrops adjacent to the low-flow channel were manually digitized from the 2010 orthophoto at a scale of 1:1,000.

Table 6.   Elevation classification criteria and mapping schemas, derived from detrending a 2010 digital elevation model (Woolpert, Inc., 2010), used to delineate geomorphic features based on their elevation relative to the local low-flow water surface of Klamath River, California.

[See companion data release (Curtis and Bond, 2020) for additional details. **Abbreviations**: RKM, river kilometer; ft, foot; IGD, Iron Gate Dam gage; SEIAD, Seiad Valley gage; >, greater than]

Relative elevation upstream from RKM 71 (ft)	Relative elevation downstream from RKM 71 (ft)	Geomorphic feature	IGD stage (ft)	SEIAD stage (ft)	Inundation frequency
0	0	Wetted channel	0	0	Low-flow
4	4	Low bar	3	4	Q2
6	8	High bar	8	9	Q5
10	13	Floodplain	11	22	Q10
15	20	Uplands	>14	>22	>Q10

The REM was used to determine inundation extents and frequencies despite longitudinal variations in water depths produced by channel constrictions and expansions, changes in flow resistance, the presence of alluvial features, and tributary confluences. In short, features located at higher elevations (floodplains) are inundated less frequently, and lower elevation features (bars) are inundated more frequently.

In theory, geomorphic features are created and maintained by a specific discharge that is regularly repeated. The relative elevations used in the mapping schema were correlated to gage heights for specific discharges at the two study gages (table 6). The current stage-discharge relations were then used to determine the magnitude of flows that inundate different geomorphic surfaces.

Inundation frequencies for specific discharges were estimated using a recent flood-frequency analysis (table 2) and correlated to the mapping schema. Generally, low bars are inundated by flows with a recurrence interval of greater than or equal to 2 years (Q2), high bars by flows with a recurrence interval of greater than or equal to 5 years, and floodplains by flows with a recurrence interval of greater than or equal to 10 years. Flood-inundation boundaries were created by merging the geomorphic features inundated by the Q2, Q5 and Q10 flows.

Sediment storage in bars and floodplains was summarized longitudinally along the main-stem river corridor for 1-km reaches, which represents the maximum length recommended for reach-scale physical habitat characterization in non-wadeable streams (Fitzpatrick and others, 1998). Areas recessed within tributary valleys were excluded from the summary analysis.

Riparian Vegetation and Flood-Induced Scour

High resolution three- and four-band imagery from the National Agriculture Imagery Program (NAIP; https://gis.apfo.usda.gov/arcgis/rest/services) collected in 2005, 2009, and 2016 (table 3) were used as the base for mapping riparian vegetation. The imagery was clipped to the study area boundary to isolate the area of interest along the main-stem river corridor and imported into eCognition (v.9.4.0) for pre-processing and vegetation classification.

Pre-processing included creating two vegetation indices: the Normalized Difference Vegetation Index (NDVI; Tucker, 1979) and the Normalized Difference Water Index (NDWI; McFeeters, 1996). These vegetation indices measure reflectance differences across the light spectrum. For example, NDVI uses the normalized difference of red and near-infrared (NIR) bands to measure photosynthetic activity or "greenness" (Carlson and Ripley, 1997). The NDWI, which uses green and NIR band contrasts that maximize water feature identification, was used to classify and remove the wetted channel and other water bodies to allow for a more accurate classification of the vegetation.

Once the water bodies were removed, vegetation was classified using an object-based classification, an image classification algorithm applied to groups of pixels or "objects" (Yu and others, 2006). In this case, the objects represent features on the ground, such as uniform stands of vegetation or bare ground. Similar to other types of image classification, object-based classification divides an image into a set of discrete classes on the basis of training datasets. This method is advantageous when using classification hierarchies that include vegetation types that may be difficult to distinguish from one another.

The eCognition learning database was used to create objects within similar spectral characteristics using a process referred to as "segmentation." A random forest (RF) classification was used to classify the segmented objects. Random forest classification is a machine-learning method that generates a multitude of random decision trees that are then iteratively aggregated to compute a classification (Liaw and Wiener, 2002).

An RF model was trained and tested using randomly selected segments that were categorized into a shadow class, three vegetation classes (trees, shrubs, grass), and a bare ground class. Classes for the training dataset were determined on the basis of field surveys collected in October of 2019 and image interpretation. During image interpretation, segment classes were defined by consensus between two independent analysts. The randomly selected segments were then subdivided into training and test datasets, which were used to train the RF model and independently test the accuracy of the results.

Map accuracy metrics included Producer's accuracy (1-omission error), User's accuracy (1-commission error), and overall accuracy for the 2005, 2009, and 2016 maps calculated using independent datasets. The Producer's accuracy is calculated as the percent of on-the-ground test samples for a given class that are accurately classified. The User's accuracy is calculated as the percent of mapped segments for a given class that are classified correctly.

A change detection analysis for two periods (2005 to 2009; 2009 to 2016) was completed to assess vegetation changes following the 2006 scour event and during a multi-year drought. To investigate vegetation changes, the grass, trees, and shrubs classes were combined into a single vegetation class. Stripping of vegetation from bars and floodplains, identified as a change from vegetated to bare ground, was interpreted as scour. A change from bare ground to vegetation was interpreted as vegetation recovery.

The 2005, 2009, and 2016 vegetation maps and metadata were published separately (Poitras and Byrd, 2020). Changes in vegetation were summarized longitudinally along the river corridor for 1-km reaches. Analysis of changes in vegetation cover was conducted within the Q10 floodplain-inundation boundary. Areas recessed within tributary valleys were excluded from the summary analysis.

Findings

Within the study reach, the main-stem Klamath River is a partially alluvial channel, frequently constrained by bedrock, and not self-formed within a floodplain. Channel confinement precludes active channel migration and non-alluvial reaches typically exhibit steep channel margins. In alluvial reaches with low elevation bars, channel margins have a gradual, ramped morphology.

The magnitude of the physical processes that create and maintain an ecologically functional river corridor increase downstream, along with sediment supply and streamflow. Increases in sediment supply or decreases in transport capacity within the study reach correspond to areas that also exhibit increases in sediment storage. The relation between sediment supply and transport capacity plays a key role in bed mobility and channel dynamics (Dietrich and others, 1989). Sediment-rich reaches are more likely to have greater areas of full mobility, sediment-poor reaches are more likely to have greater areas of partial transport, and both sediment-supply regimes can have substantial areas that are essentially immobile (Lisle and others, 2000).

Sediment Mobility

Within the study reach, the history of sediment-mobilization flows can be split into three periods (fig. 6): (1) a historical wet period from 1964 to 1999 when sediment-mobilization flows were common; (2) a historical dry period from 2000 to 2015, which included the 2012–16 drought, when sediment-mobilization flows were rare; and (3) a recent moderately wet period from 2016 to 2019 when court-mandated flows were implemented. During the recent period, surface-flushing and deep-flushing thresholds, as defined by Shea and others (2016), were exceeded in 3 out of 4 years, which represents a return to flushing-flow frequencies that mimic conditions during the historical wet period.

From 1964 to 1999, the recurrence interval for surface-flushing flows was 2 years, which is consistent with free-flowing rivers. During the drier second period, the interval between surface flushing flows increased to 4 years, and during the recent period, the interval was 1–2 years. In comparison, the recurrence interval for deep-flushing flows during the historical wet period was 2 years, which increased to 16 years during the drier second period and returned to 1–2 years during the recent period.

In contrast, from 1964 to 1999, the recurrence intervals for armor-disturbing and geomorphically effective flows were 5 and 7 years, respectively. These higher flows have not occurred since water year 1997 and during the recent period, the average interval between large channel maintenance flows increased to more than 20 years (fig. 3).
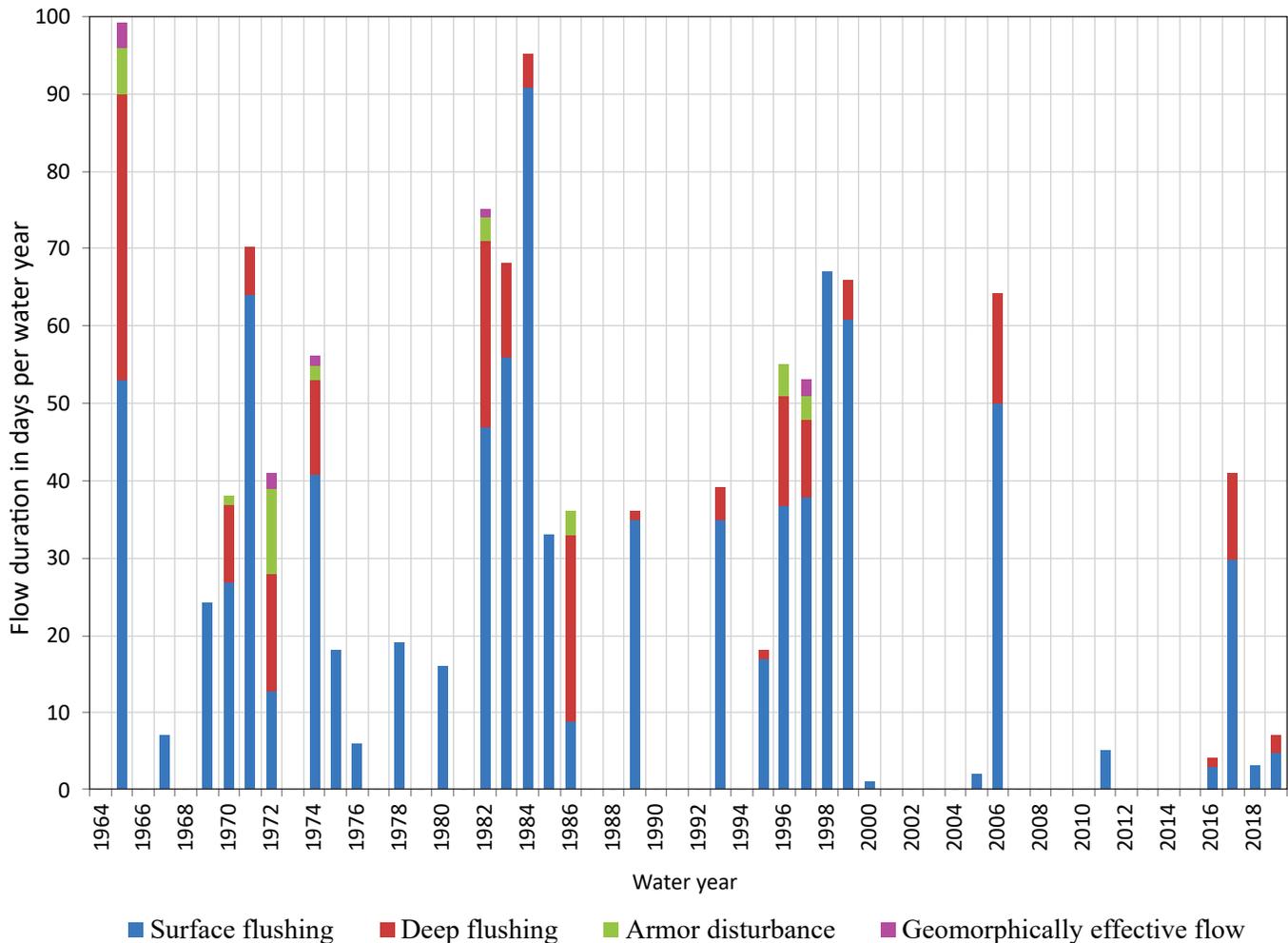


Figure 6.   Duration of sediment-mobilization flows defined by Shea and others (2016) for the Klamath River below Iron Gate Dam, California (USGS gage 11516530), for water years 1965–2019. (Data available at https://waterdata.usgs.gov/nwis)

Active Sediment Transport at Two Gaged Sites

Between 2016 and 2019, there were 43 discharge measurements made at the Iron Gate gage (table 1.1) and 44 measurements made at the Seiad Valley gage (table 1.2) using ADCPs with bottom tracking. These were routine monthly discharge measurements. During reservoir releases, which typically occur in March or April, the routine measurements were timed to coincide with reservoir releases. Moving-bed tests indicate the initiation of sediment transport, on or near the bed by flows greater than 5,200 to 6,000 cubic feet per second (ft^3/s) at the Iron Gate gage and greater than 7,700 to 8,800 ft^3/s at the Seiad Valley gage (fig. 7). The direct measurement of moving-bed conditions provides an estimate of the critical discharge necessary to initiate sediment movement at the two study gages. These critical discharges were used to define sediment-mobilization thresholds for each of the study gages that validate proposed flow thresholds for sediment mobilization (table 7).

An important caveat for interpreting the bed mobility data is that the presence of a moving bed is dependent on sediment-supply and local hydraulic conditions at the measurement cross-section. For these reasons, moving-bed conditions can vary in time and space and may not always be present at a given discharge. In addition, bed mobility is frequently restricted to the rising limb of the hydrograph (Schmidt and Potyondy, 2004; Gendaszek and others, 2017) and the lack of a moving bed does not indicate that the bed was stationary before the measurement. Under supply limited conditions, mobile bed-material may have been transported past the cross section before the measurement. To address the caveats that produce the variability shown in figure 7, repeat measurements may be required during natural runoff events and reservoir releases to characterize the temporal variability of mobile bed conditions and to reduce uncertainty.

Between 2005 and 2019, changes in mean bed elevations were estimated using 116 discharge measurements made at the Iron Gate gage and 83 measurements made at the Seiad Valley gage (fig. 8). Variability in the time series, interpreted as localized scour and fill, provided indirect evidence of active sediment transport within the gaged reaches.

The 2006 scour event at the Seiad Valley gage, with a peak flow magnitude of 74,000 ft^3/s and recurrence interval of greater than 10 years (table 2), resulted in approximately 1.0 ft of bed degradation between discharge measurements made on December 7, 2005, and July 6, 2006. Since 2006, smaller magnitude flows with recurrence intervals of 2–5 years (table 2) produced episodic scour and fill that resulted in synchronous, but transient, changes in mean bed elevations at both gages.

Surface Flushing of Fine-Sediment at Two Ungaged Sites

In 2017 and 2018, small patches of fine sediment (less than 2 mm in diameter) and larger lobate-shaped deposits of loose gravel and cobble were present at the two ungaged sites (KCC and PC; fig. 4). The surface samples contained less than 5-percent fines and subsurface samples contained less than 22-percent fines (tables 8, 9; fig. 9). The scarcity of surface fines in the vegetated (less than 5 percent) and unvegetated (less than 4 percent) plots was similar. A previous study (Holmquist-Johnson and Milhous, 2010) documented similar bed conditions following the 2006 scour event, where fines were present in the subsurface but scoured from the surface. Bed substrate composition is an indicator of the balance between sediment supply and transport capacity (Dietrich and others, 1989). A lack of surface fines and the presence of a coarse armor layer suggests excess transport capacity for fines.

Sediment samples were collected in September of 2018 following the peak flow in 2017 (fig. 3), which had a recurrence interval of more than 5 years (table 2). Results indicate the 2017 peak flows, with a magnitude of 10,400 ft^3/s at the Iron Gate gage and 43,000 ft^3/s at the Seiad Valley gage, scoured fine sediment from the surface of low bars at the two ungaged sites. In 2017, at the Iron Gate gage, mean daily flows exceeded the surface-flushing threshold of 8,700 ft^3/s for 30 days and exceeded the deep-flushing threshold of 11,250 ft^3/s for 11 days (table 1; fig. 6).

Table 7.   Flow thresholds for initiating bed mobility at two U.S. Geological Survey (USGS) gaging stations, Klamath River, California. (See fig. 4 for gage location and table 2 for gage descriptions.)

[ft³/s, cubic foot per second; IGD, Iron Gate Dam gage; SEIAD, Seiad Valley gage; ±, plus or minus; NA, not applicable]

USGS station number	USGS station name	Station identifier	This study (ft³/s)	Ayres and Associates, 1999 (ft³/s)	Bureau of Reclamation, 2011 (ft³/s)	Holmquist-Johnson and Milhous, 2010 (ft³/s)
11516530	Klamath River below Iron Gate Dam, CA	IGD	5,200–6,000	5,400	6,900	5,000
11520500	Klamath River near Seiad Valley, CA	SEIAD	7,700–8,800	6,600	15,300	NA
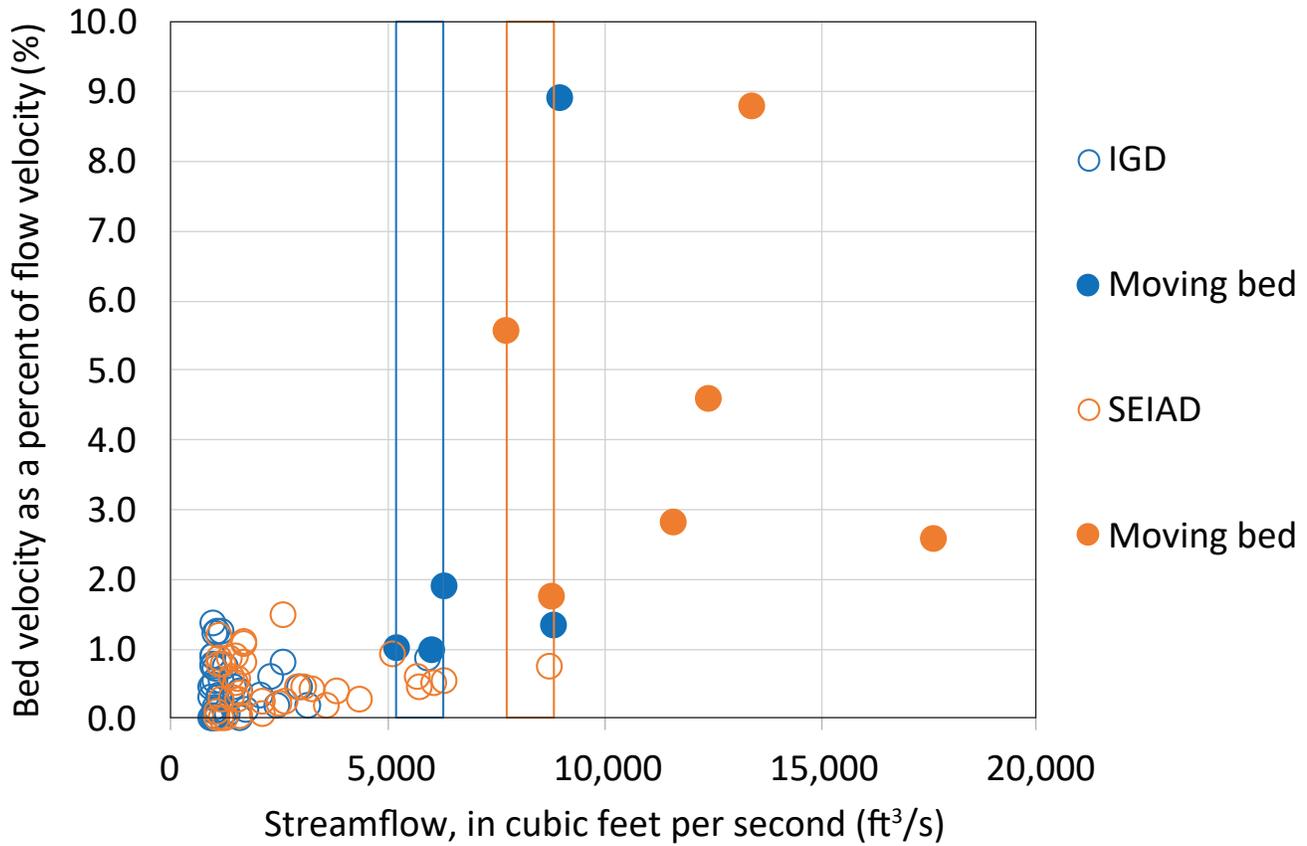
Figure 7.   Relation of streamflow rate to bed velocity as a percentage of flow velocity, defined as percent moving bed, for cross-sectional discharge measurements made using an acoustic Doppler current profiler with bottom tracking at two U.S. Geological Survey (USGS) gaging stations: Klamath River below Iron Gate Dam, CA (IGD; USGS 11516530) and Klamath River near Seiad Valley, CA (SEIAD; USGS 11520500) during water years 2016–19. (Boxes delineate sediment mobility thresholds defined at 5,200–6,000 ft³/s for IGD and 7,700–8,800 ft³/s for SEIAD. See fig. 4 for gage locations and table 2 for gage descriptions.)

A.

B.
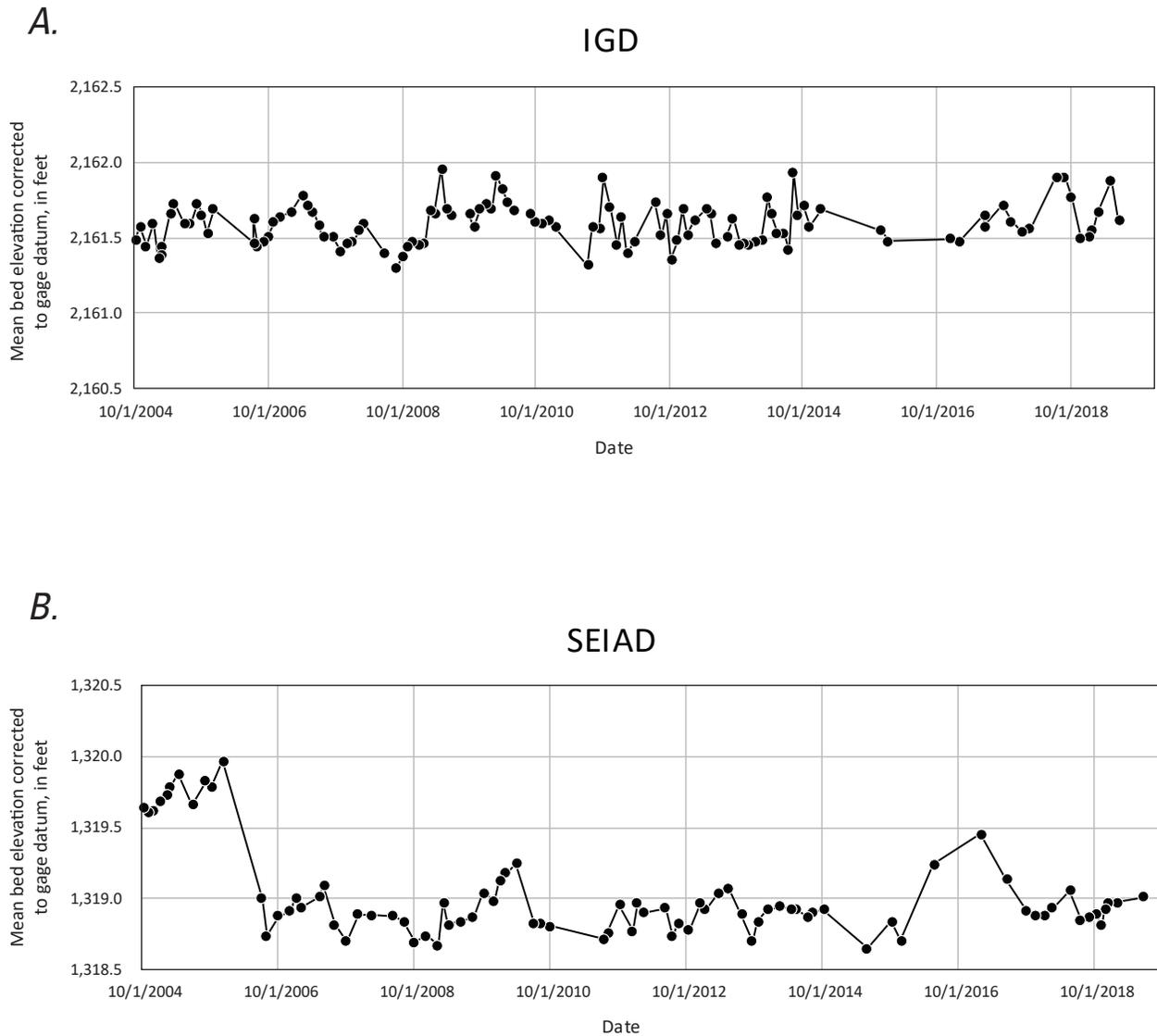
Figure 8. Changes in mean bed elevation relative to the National Geodetic Vertical Datum of 1929 (NGVD 29) at two U.S. Geological Survey (USGS) gaging stations for *A*, Klamath River below Iron Gate Dam, CA (IGD; USGS 11516530); and *B*, Klamath River near Seiad Valley, CA (SEIAD; USGS 11520500), estimated using discharge measurements made during water years 2005–19. (Data available at https://waterdata.usgs.gov/nwis. See fig. 4 for gage location and table 2 for gage descriptions.)

Table 8.   Grain size analysis for bulk sediment samples collected in September 2018 at Klamath Community Center (KCC) located 53 kilometers downstream from Iron Gate Dam along the main-stem Klamath River, California.

[See figure 3 for site location. **Abbreviation**: mm, millimeters]

Grain size (mm)	Percent less than					
	KCC1 low bar dense vegetation SURFACE	KCC1 low bar dense vegetation SUBSURFACE	KCC2 low bar dense vegetation SURFACE	KCC1 low bar no vegetation SURFACE	KCC1 low bar no vegetation SUBSURFACE	KCC2 low bar no vegetation SURFACE
Cobble						
128	100.00	100.00	100.00	100.00	100.00	100.00
90	100.00	100.00	100.00	72.91	100.00	54.41
Gravel						
64	72.37	94.21	100.00	39.63	91.65	31.87
45	43.63	76.85	63.28	27.24	80.85	26.63
29	25.95	59.50	39.51	13.31	65.63	20.34
23	13.79	47.92	27.63	7.89	51.38	14.58
16	8.27	37.51	17.91	5.57	43.04	10.91
11.2	4.95	29.41	12.51	4.02	33.71	7.76
8	2.74	23.62	8.19	3.25	27.81	5.67
4	2.74	23.52	6.03	2.47	22.84	4.09
Sand						
2	1.43	17.23	3.99	1.55	16.52	2.57
1	0.84	12.28	2.83	0.98	10.51	1.60
0.5	0.47	8.28	2.27	0.68	5.62	1.05
0.25	0.27	5.49	1.89	0.55	3.41	0.84
0.125	0.12	2.06	1.08	0.27	1.64	0.41
Silt and clay						
0.062	0.06	0.72	0.39	0.11	0.68	0.16
0.03	0.02	0.24	0.10	0.05	0.30	0.06

Table 9.   Grain size analysis for bulk sediment samples collected in September 2018 at Portuguese Creek (PC) located 104 kilometers downstream from Iron Gate Dam along the main-stem Klamath River, California.

[See figure 3 for site location. **Abbreviation**: mm, millimeters]

| Grain size (mm)	Percent less than					
	PC1 low bar dense vegetation SURFACE	PC1 low bar dense vegetation SUBSURFACE	PC2 low bar dense vegetation SURFACE	PC1 low bar no vegetation SURFACE	PC1 low bar no vegetation SUBSURFACE	PC2 low bar no vegetation SURFACE
Cobble						
128	100.00	100.00	100.00	100.00	100.00	100.00
90	75.89	100.00	88.19	74.91	87.21	64.86
Gravel						
64	55.33	100.00	39.24	56.24	84.84	38.22
45	31.22	89.68	17.30	40.49	68.73	18.95
29	17.75	79.36	8.86	27.07	58.78	10.45
23	13.49	64.92	6.04	18.90	50.25	6.48
16	10.65	56.66	4.36	13.65	44.09	3.65
11.2	8.53	48.41	3.23	9.57	36.51	1.95
8	7.11	41.19	2.67	7.24	30.82	1.38
4	5.65	33.96	2.07	6.01	26.56	0.81
Sand						
2	3.82	22.34	1.39	4.72	19.15	0.59
1	2.39	13.19	0.99	3.68	12.82	0.52
0.5	1.72	9.55	0.84	3.20	8.76	0.50
0.25	1.36	7.48	0.72	2.93	7.26	0.46
0.125	0.63	3.13	0.40	1.88	4.16	0.33
Silt and clay						
0.062	0.31	1.37	0.20	0.93	1.99	0.20
0.03	0.13	0.57	0.08	0.36	0.86	0.09

A.
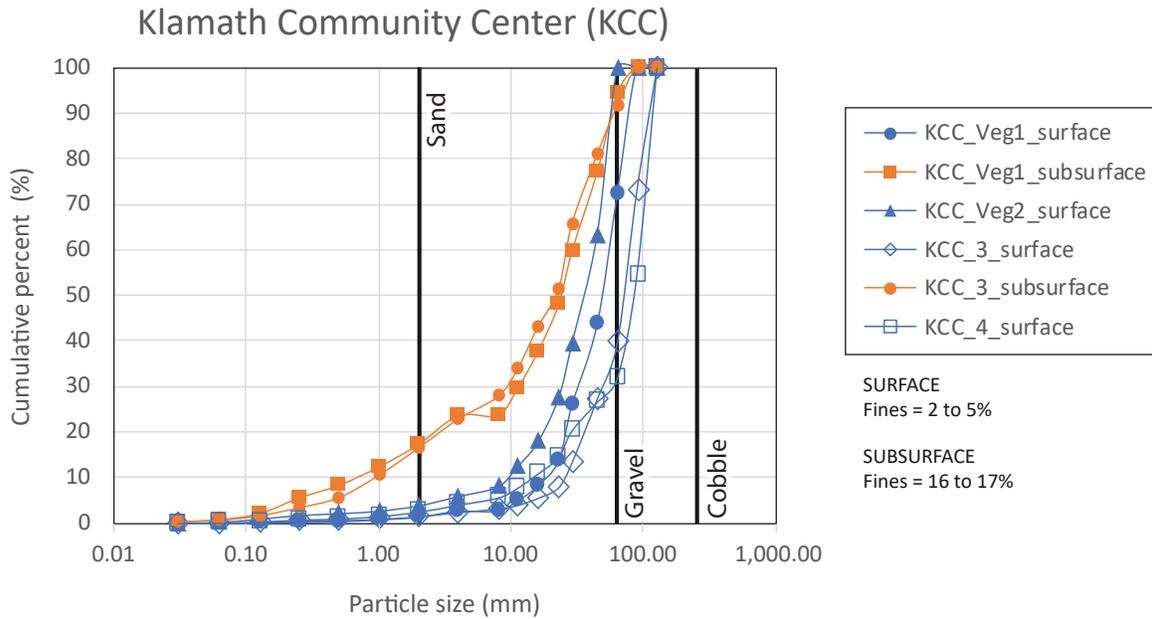
B.
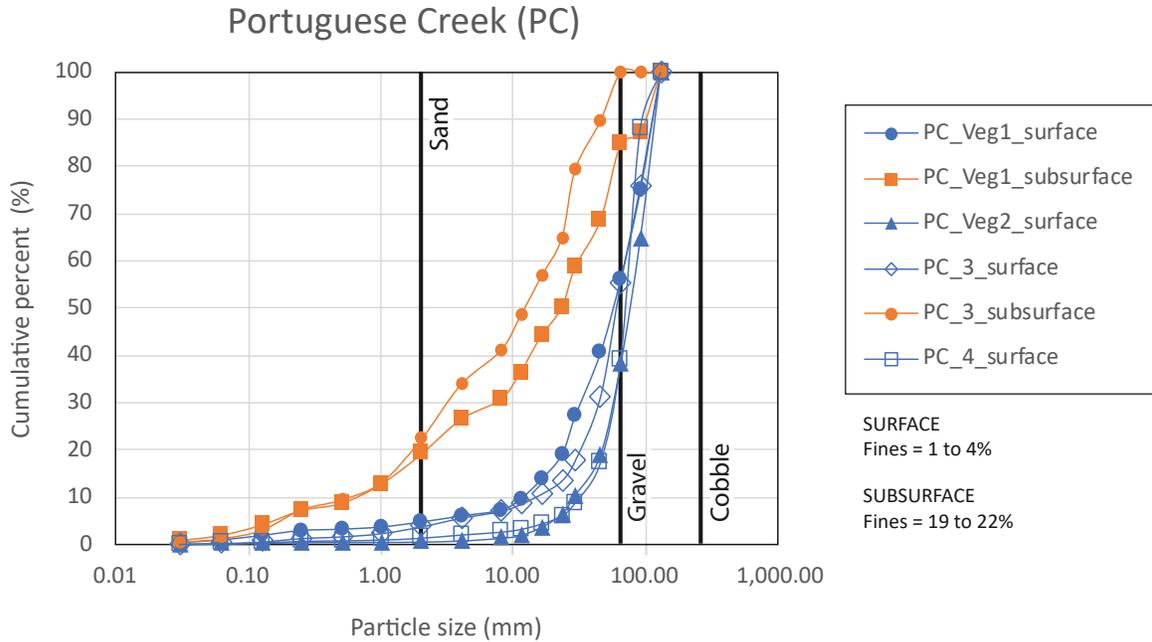
Figure 9.   Substrate grain-size distributions for bulk surface and subsurface samples collected from low elevation bars in vegetated and unvegetated plots collected in September 2018 at two ungaged sites along the main-stem Klamath River below Iron Gate Dam, California. (See fig. 4 for site locations. Data available in tables 8 and 9.)

Riparian Corridor Assessment

Previous studies (Ayres and Associates, 1999; PacifiCorp, 2004) suggested that riparian vegetation patterns have remained constant and concluded that changes in the river's flow regime related to water management produced no significant changes in channel morphology. In this study, higher-resolution datasets enabled an assessment of sediment storage and changes in vegetation along narrow, discontinuous alluvial margins that are well vegetated (fig. 10).

Longitudinal Summary of Sediment Storage

In the presence of a well-defined cut bank, the relative elevation model accurately delineated the transition between alluvial features. Often, however, the transition between low bars and high bars was poorly delineated solely on the basis of the relative elevation model, and the polygon boundaries for these features required extensive manual editing.

Bar and floodplain dimensions are fundamentally influenced by the magnitude and frequency of inundation and the balance between sediment supply and transport capacity. Example geomorphic maps (fig. 11) show the juxtaposition of the channel and riparian features (table 4). Sediment storage in bars and floodplains within 1-km reaches was summarized longitudinally (fig. 12*A*) and cumulatively (fig. 12*B*) by discrete reaches.

Sediment storage increases downstream from Beaver Creek (RKM 48), which suggests a transition from supply limited to equilibrium or transport-limited conditions. Reach-averaged channel widths (fig. 13) estimated using the Q2, Q5, and Q10 flood-inundation boundaries also increase downstream from RKM 48. Two-tailed t-tests of mean widths upstream and downstream from RKM 48 indicate a statistically significant difference in mean channel widths for the Q2 (p-value less than 0.0001), Q5 (p-value less than 0.0001), and Q10 (p-value equal to 0.0014) boundaries even without the influence of large alluvial features upstream of the Seiad Valley gage (RKM 102). This transition is also apparent on the longitudinal profile (fig. 4), which shows an aggradational reach between Beaver Creek (RKM 48) and the Seiad Valley gage (RKM 102).

Changes in Riparian Vegetation Following Flood Disturbance

The overall accuracies for the RF models for the 2005, 2009, and 2016 vegetation maps were 85, 89, and 84 percent, respectively (table 10). User's accuracy, which is the percent of segments mapped correctly, for bare ground exceeded 92 percent for all 3 years. Producer's accuracy, which is the percent of on-the-ground test samples for a given class that are accurately classified, exceeded 81 percent for all 3 years. Of the misclassified segments for bare ground, roughly half were dirt roads not located within the Q10 flood-inundation boundary used to interpret vegetation changes. Producer's accuracy for the grass category was low in 2016, at 72 percent, because of confusion with shrubs but exceeded 89 percent for 2005 and 2009. User's accuracy for the grass category exceeded 80 percent for all 3 years.

The time series of vegetation maps document the response of riparian vegetation to flood disturbance caused by the 2006 scour event and subsequent recovery during a drier period that included the 2012–16 drought. Example vegetation maps illustrate the shadow, bare ground, and three vegetation classes for a selected reach downstream from Beaver Creek (fig. 14). Response times for reestablishment vary by plant species, which was not addressed in this study.

The areal extent of bare ground, water, and vegetation in 2005, 2009, and 2016 were summarized longitudinally along the river corridor at 1-km intervals (fig. 15). A comparison of the 2005 and 2016 maps indicate the largest changes in riparian vegetation occurred at tributary confluences, with notable changes at RKM 5 (Little Bogus Creek), RKM 31 (Humbug Creek), RKM 48 (Beaver Creek), RKM 53 (Little Humbug Creek), RKM 71 (Horse Creek #1), RKM 78 (Scott River), RKM 99 (Grider and Seiad Creeks), and RKM 125 (Horse Creek #2).

From 2005 to 2009, bare ground upstream from the Scott River (RKM 78) increased and vegetation cover decreased, which indicated stripping of vegetation from bars and floodplains during the 2006 scour event. Higher water in 2009, during orthophoto acquisition (table 3), precluded an assessment of changes downstream from RKM 78. During the 2006 scour event, streamflow peaked at the Iron Gate gage at 12,400 ft^3/s and 74,000 ft^3/s at the Seiad Valley gage and streamflow at the Iron Gate gage was above the deep-flushing flow threshold for a total of 14 days (fig. 6). The 2006 scour event had a recurrence interval of greater than 5 years at the Iron Gate gage and greater than 10 years at the Seiad Valley gage (table 2).

From 2009 to 2016, the area of bare ground decreased and vegetation cover increased upstream from the Scott River (RKM 78), which indicated reestablishment of riparian vegetation following the 2006 scour event when lower flows during a drier period facilitated vegetation recovery. From 2009 to 2016, the mean daily flow at the Iron Gate gage remained below the surface-flushing threshold, with one exception. During water year 2011, flows exceeded the surface-flushing threshold for 5 days (fig. 6).

Figure 10.   U.S. Fish and Wildlife employee and a substrate grain-size plot (KCC_Veg1), showing evidence active bedload transport along a densely vegetated channel margin, collected in September 2018 at Klamath Community Center (KCC), located 53 kilometers downstream from Iron Gate Dam along the main-stem Klamath River, California. (See fig. 9 and table 8 for grain size distributions and fig. 4 for site location). Photograph taken by Jennifer Curtis, U.S. Geological Survey.

During the study period from 2005 to 2016, flows with recurrence intervals of 5–10 years (table 2) stripped vegetation from bars and floodplains upstream from the Scott River. A previous study (Ayres and Associates, 1999) documented similar vegetation changes following the 1997 scour event, which removed substantial amounts of aquatic and riparian vegetation in the reach between Iron Gate Dam and the Scott River.
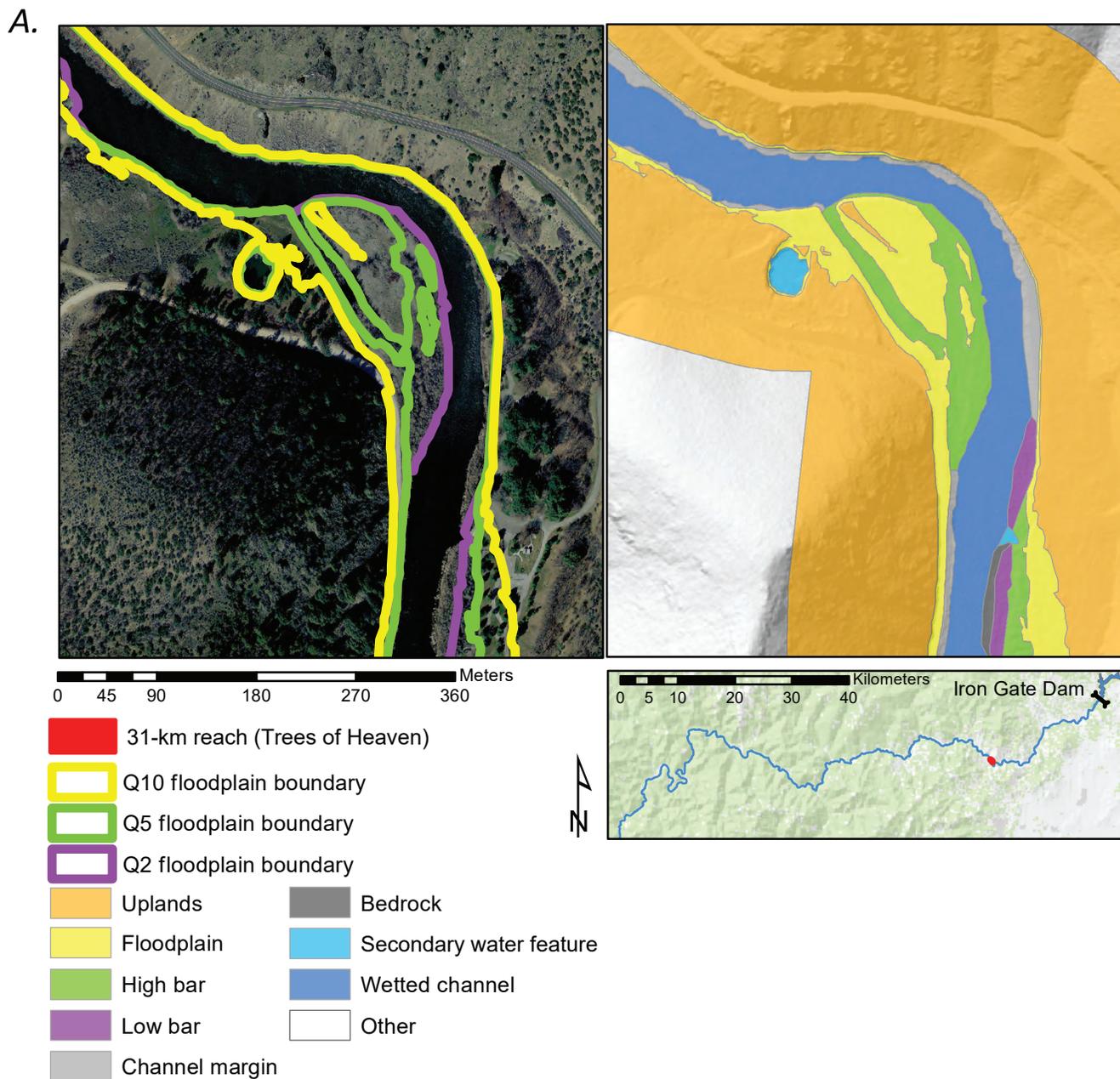
Figure 11. Reach-scale riparian and channel features along the main-stem Klamath River below Iron Gate Dam, California, 2010 for *A*, Trees of Heaven RKM 31; *B*, Klamath Community Center RKM 53; and *C*, Portuguese Creek RKM 104. Inundation extents for flows with 2-year, 5-year, and 10-year recurrence intervals are shown and were defined on the basis of the low bar (Q2), high bar (Q5), and floodplain (Q10) feature boundaries. (See table 4 for geomorphic feature definitions and companion data release [Curtis and Bond, 2020] for additional details)

B.

Meters
0   50   100   200   300   400

Kilometers
0   5   10   20   30   40   Iron Gate Dam

- 53-km reach (Klamath Community Center)
- Q10 floodplain boundary
- Q5 floodplain boundary
- Q2 floodplain boundary
- Uplands   Bedrock
- Floodplain   Secondary water feature
- High bar   Wetted channel
- Low bar   Other
- Channel margin

N

Figure 11.   —Continued

C.

Meters				
0	80	160	320	480	640

- 🟥 104-km reach (Portuguese Creek)
- 🟨 Q10 floodplain boundary
- 🟩 Q5 floodplain boundary
- 🟪 Q2 floodplain boundary
- 🟧 Uplands
- 🟨 Floodplain
- 🟩 High bar
- 🟪 Low bar
- ⬜ Channel margin
- ⬛ Bedrock
- 🟦 Secondary water feature
- 🟦 Wetted channel
- ⬜ Other

Kilometers
0 5 10 20 30 40

Iron Gate Dam

Figure 11.   —Continued

A. Areas per discrete 1-km reach
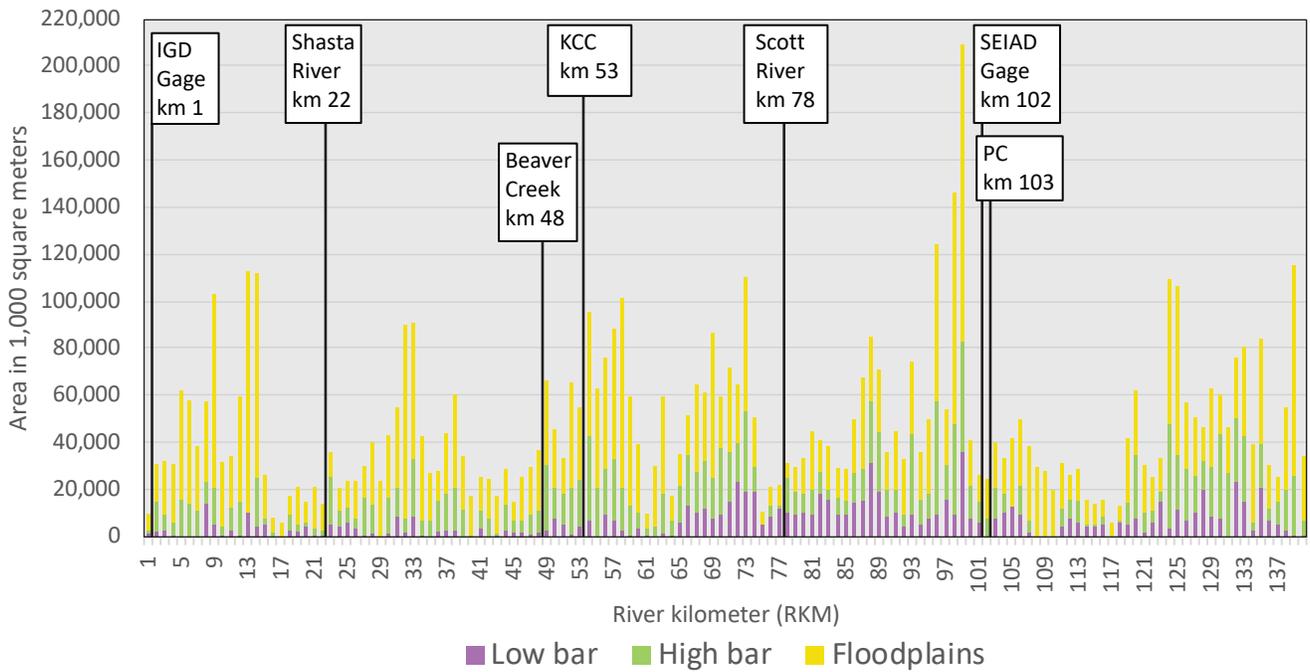
B. Cumulative area
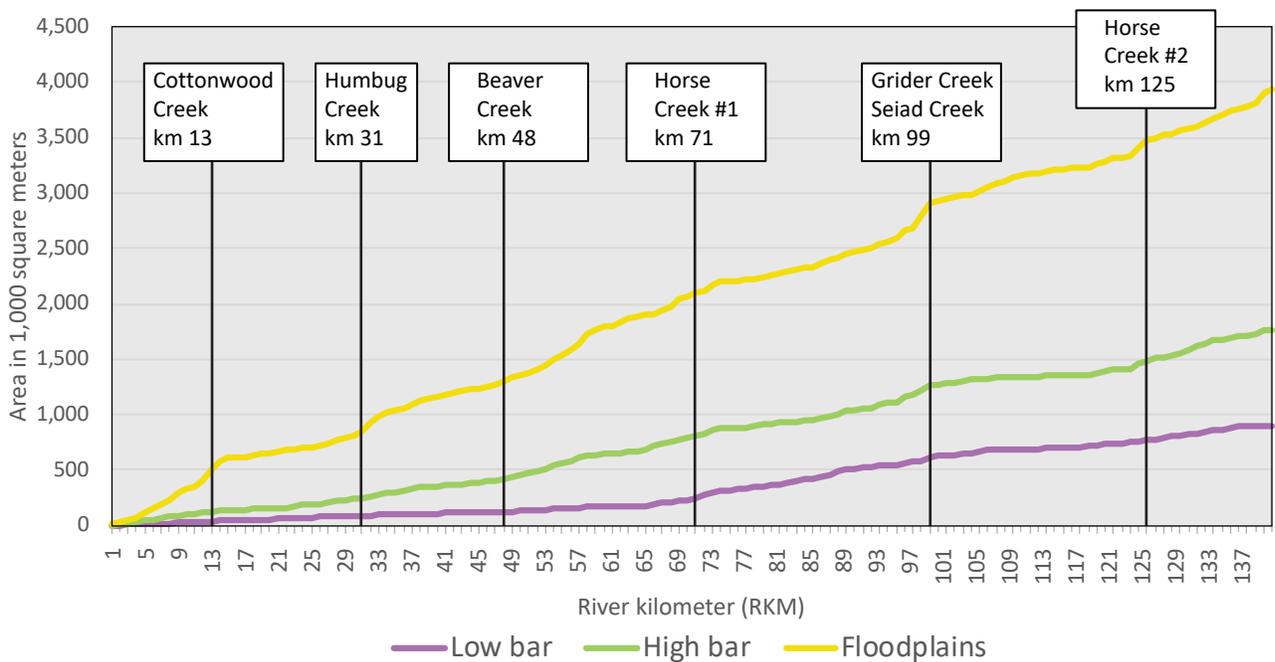
Figure 12.   Longitudinal summaries of sediment storage in bars and floodplains along 140 kilometers of the main-stem Klamath River below Iron Gate Dam, California, 2010, by *A*, area per discrete 1-km reach; and *B*, cumulative area.
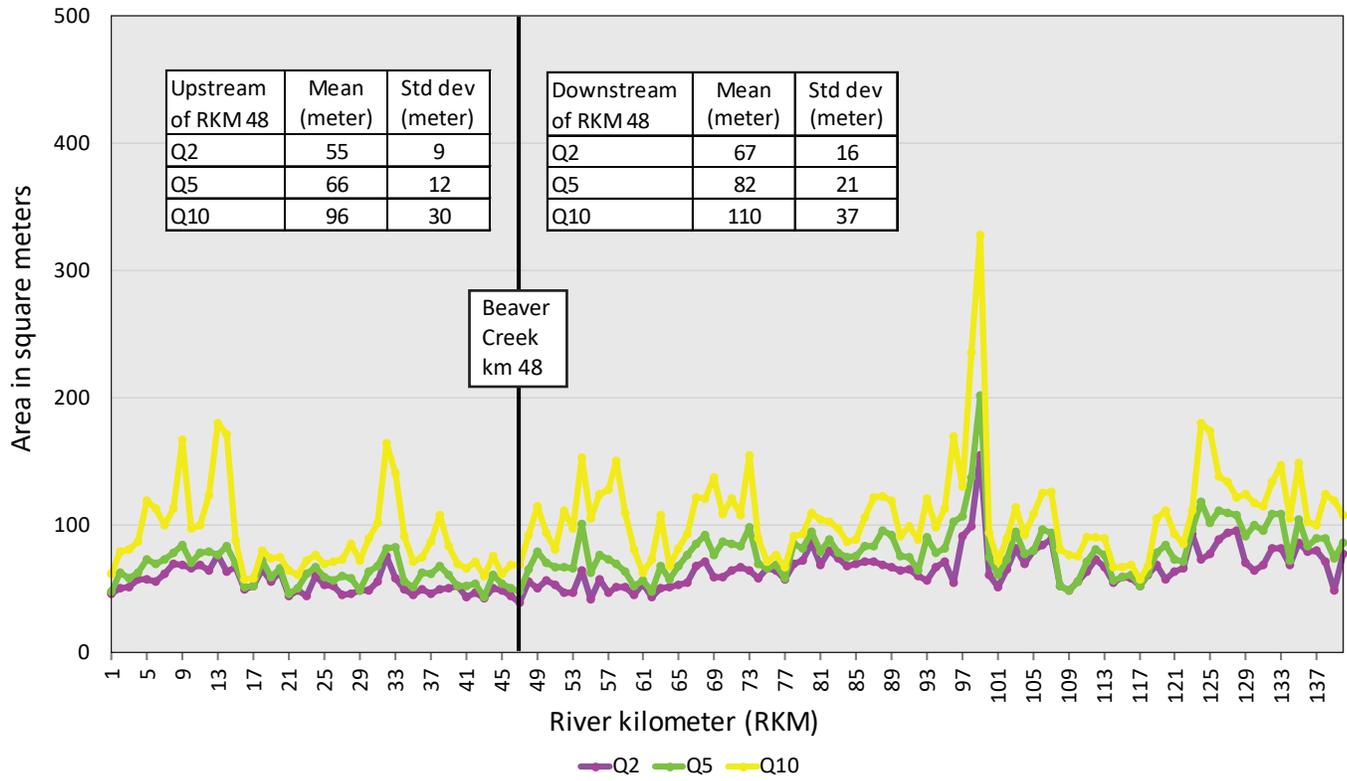
Figure 13. Reach-averaged widths of inundation boundaries for floods with recurrence intervals of 2 years (Q2), 5 years (Q5), and 10 years (Q10), along 140 kilometers of the main-stem Klamath River below Iron Gate Dam, California, 2010.

Table 10.   Confusion matrix and accuracy assessment for vegetation classification maps for 2005, 2009, and 2016, along 140 kilometers of the main-stem Klamath River below Iron Gate Dam, California.

[See companion data release (Poitras and Byrd, 2020) for additional details. **Abbreviation**: —, no data]

|	Bare ground	Grass	Shadow	Shrubs	Trees	Total	User's accuracy (percent)
2005 Overall accuracy: 85 percent							
Bare ground	70	2	0	0	0	72	97
Grass	9	72	0	3	2	86	84
Shadow	0	0	46	0	2	48	96
Shrubs	0	1	2	73	11	87	84
Trees	0	0	5	4	71	80	89
Total	79	75	53	80	86	—	—
Producer's accuracy (percent)	89	96	87	91	83	—	—
2009 Overall accuracy: 89 percent							
Bare ground	67	6	0	0	0	73	92
Grass	15	81	0	5	0	101	80
Shadow	0	0	68	0	2	70	97
Shrubs	0	1	0	72	2	75	96
Trees	1	3	6	1	54	65	83
Total	83	91	74	78	58	—	—
Producer's accuracy (percent)	81	89	91	92	93	—	—
2016 Overall accuracy: 84 percent							
Bare ground	80	0	0	0	0	80	98
Grass	13	67	0	3	0	83	81
Shadow	0	0	76	2	2	80	95
Shrubs	0	25	1	81	33	140	58
Trees	0	1	10	11	93	115	81
Total	93	93	87	97	128	—	—
Producer's accuracy (percent)	86	72	87	82	73	—	—
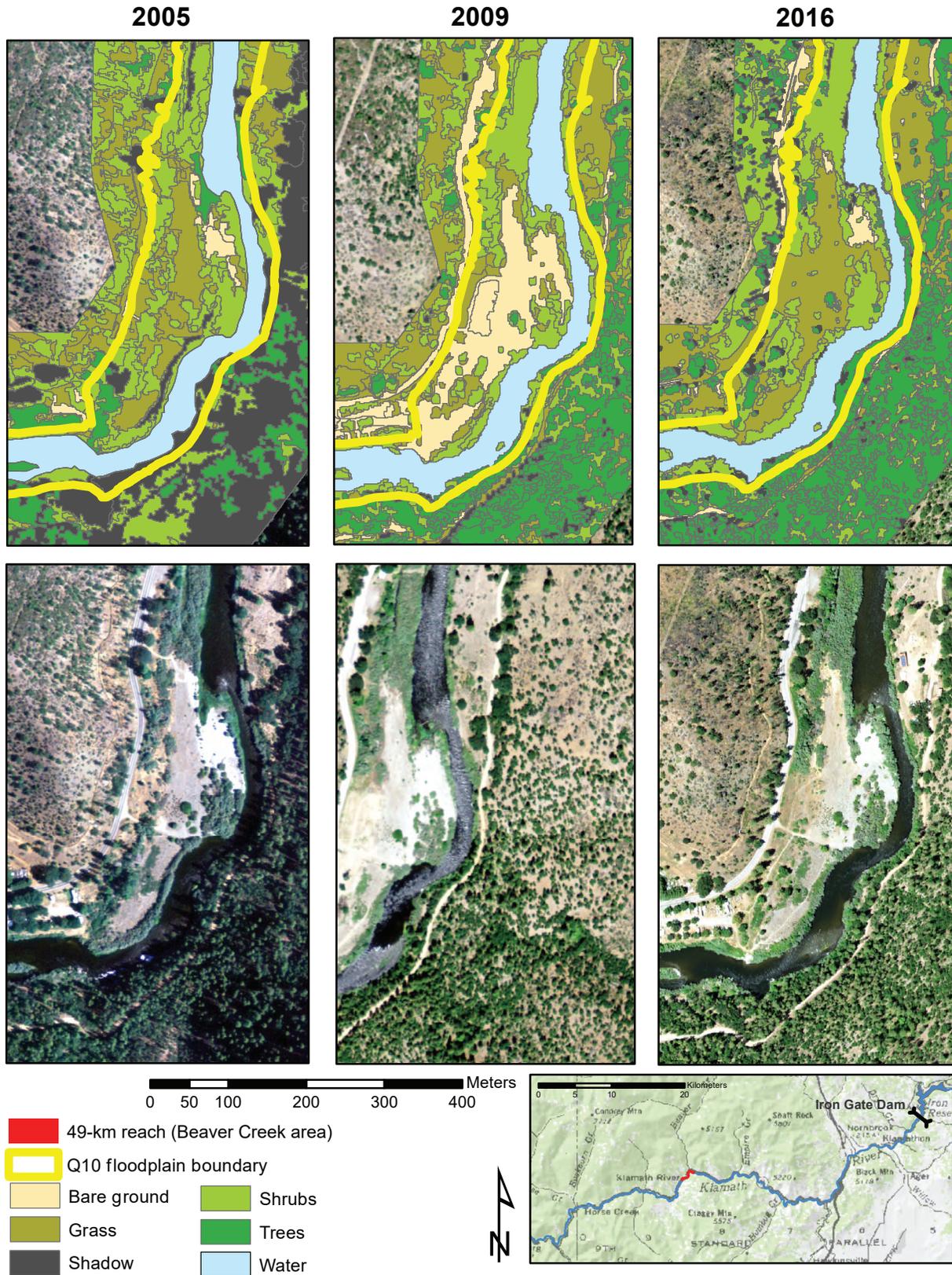
Figure 14. Example maps of riparian vegetation for 2005, 2009, and 2016 for the reach below the confluence of Beaver Creek, located 49 kilometers downstream from Iron Gate Dam along the main-stem Klamath River, California. (See companion data release [Poitras and Byrd, 2020] for additional details).

A.   2005
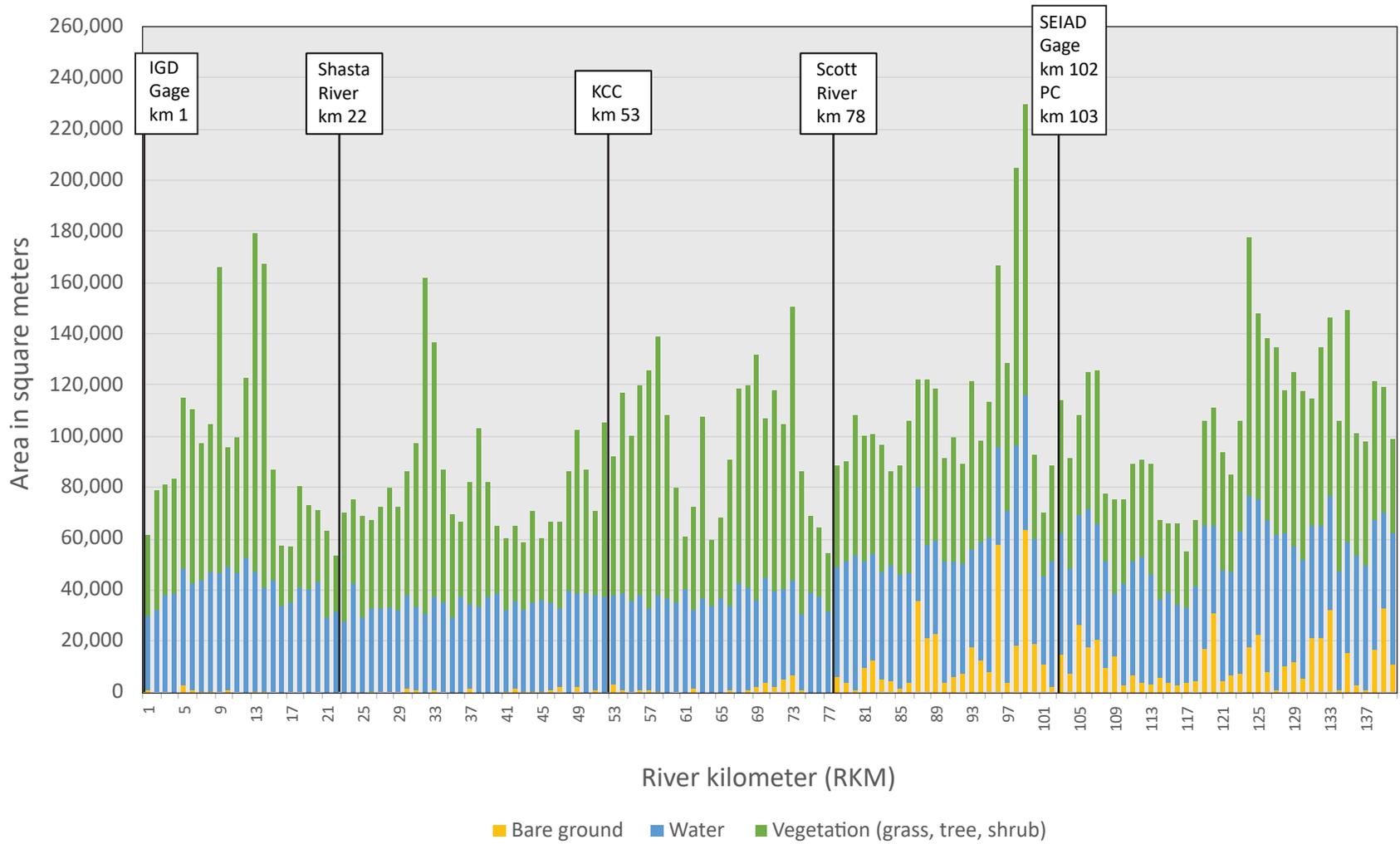
Figure 15.   Longitudinal summaries of water, bare ground, and vegetation for *A*, 2005; *B*, 2009; and *C*, 2016 within the Q10 flood-inundation boundary along 140 kilometers of the main-stem Klamath River below Iron Gate Dam, California.

B. 2009
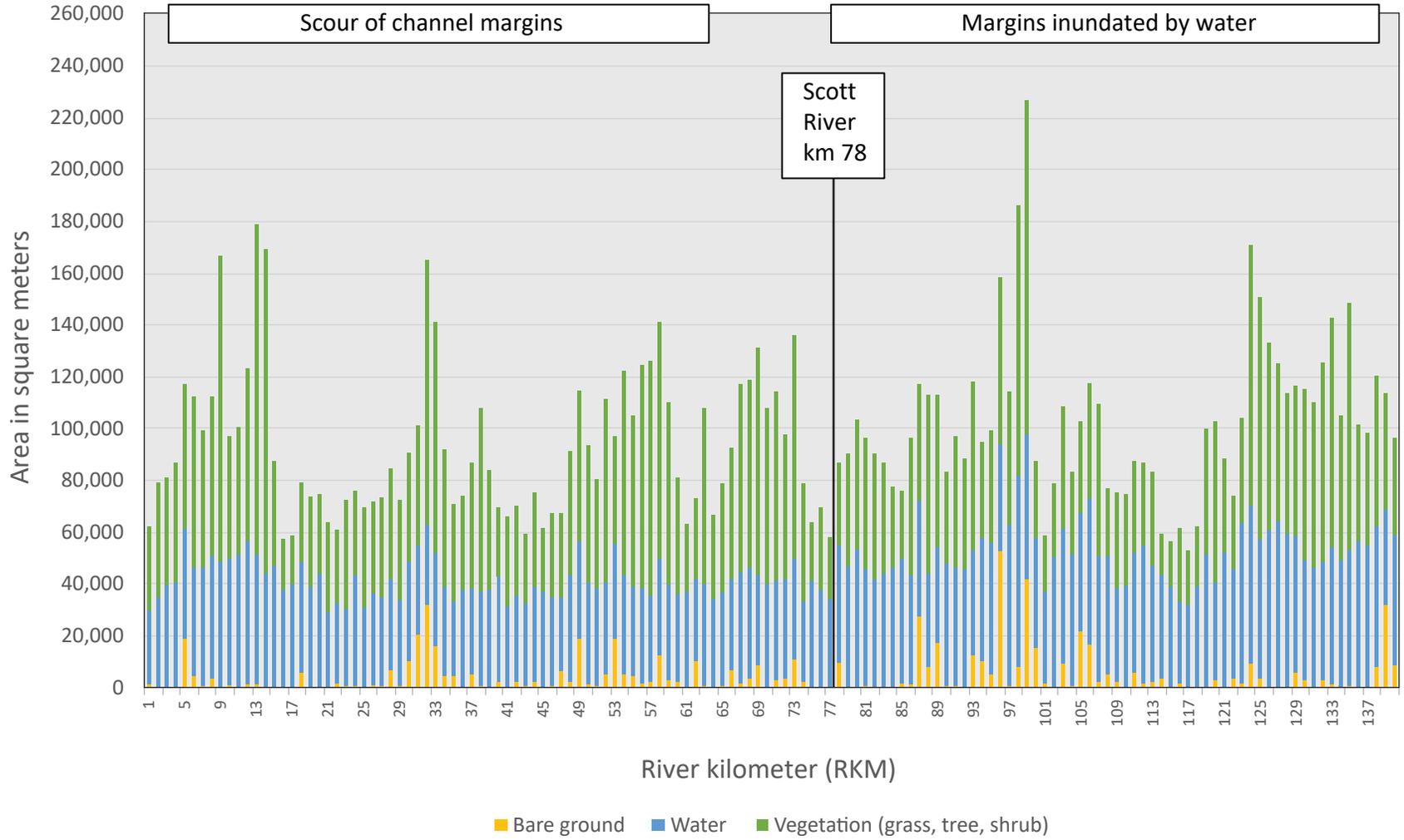
Figure 15.   —Continued
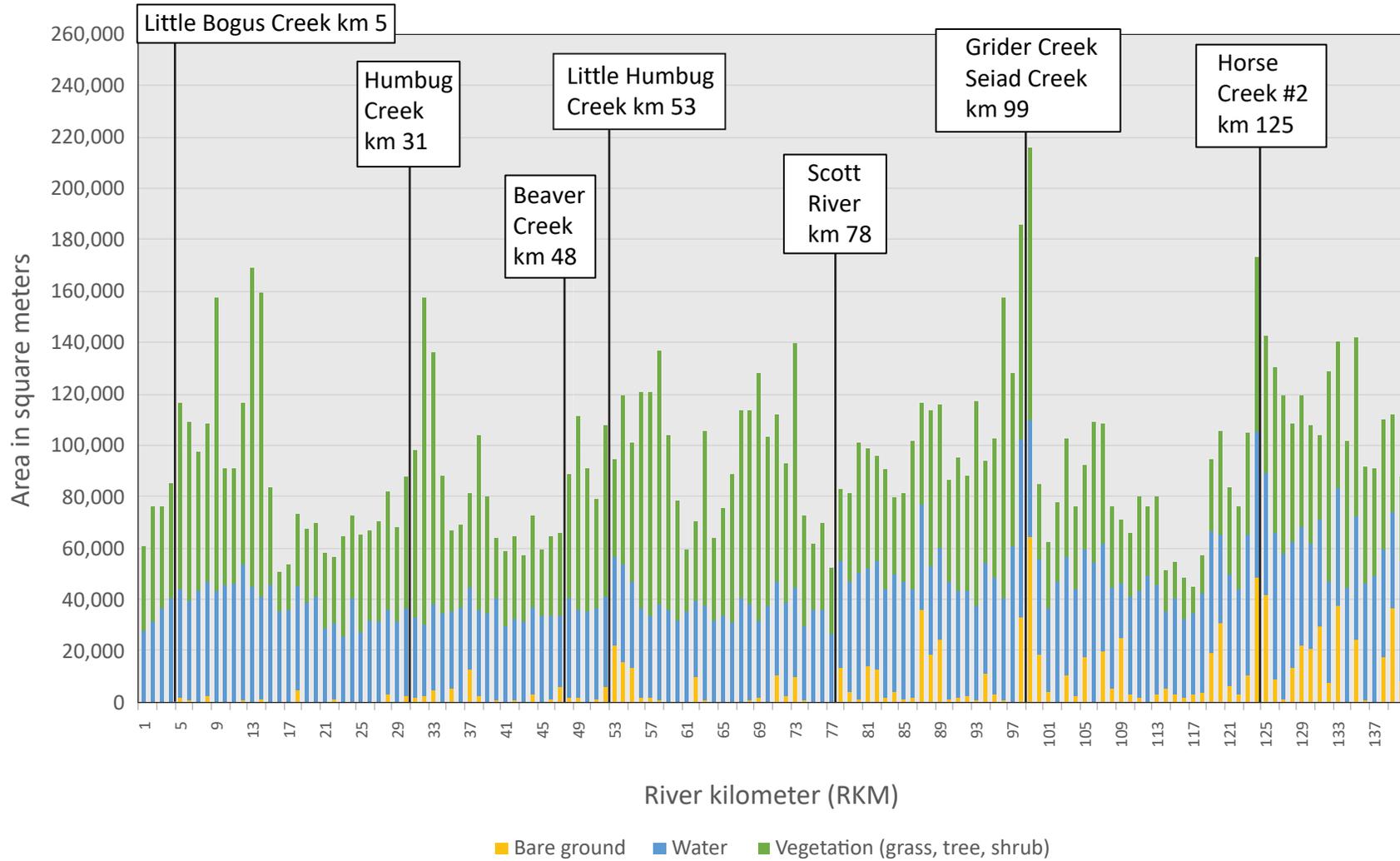
Figure 15. —Continued

Implications

Substrate conditions conducive to infectious pathogens, particularly *C. shasta*, occur periodically along the main-stem Klamath River and a key knowledge gap is whether polychaete abundance and disease prevalence can be mitigated by natural flow events or well-timed reservoir releases (Perry and others, 2019). The following is a list of high priority science studies that could fill some of the existing knowledge gaps.

- New high-resolution topo-bathymetric DEM and orthoimagery were collected in 2018. A first step toward evaluating the linkages between geomorphology, polychaete habitat, and fish disease would be to overlay polychaete abundance maps onto a 2018 geomorphology map to investigate macrohabitats and the correlation between geomorphic features and polychaete distributions as suggested by Malakauskas and others (2013).

- This study provided an estimate of sediment storage in 2010. Additional characterization of channel-maintenance flows that effectively create disturbance while maintaining a balanced sediment regime would require estimates of sediment supply, sediment storage, and the effect of flow regimes on sediment transport (Schmidt and Wilcock, 2008; Wohl and others, 2015) under existing conditions.

- The physical response of the main-stem Klamath River to channel-maintenance flows is strongly dependent upon riparian vegetation and sediment storage. The effectiveness of recent channel-maintenance flows could be further assessed by comparing the results from this study to river corridor conditions in 2018 to investigate changes in vegetation cover between 2016 and 2018 and volumetric changes in sediment storage in bars and floodplains between 2010 and 2018.

- Estimates of fine- and coarse-sediment flux would be useful for determining whether sediment-limited or transport-limited conditions exist over a range of timescales (storm, seasonal, annual).

- Monitoring the flux of fine and coarse sediment during channel-maintenance flows, released during clear water conditions when the tributaries are not flowing, would provide net flux calculations to determine the effectiveness of reservoir releases for flushing fine sediment and mobilizing coarser material.

- An investigation of floodplain connectivity would be useful for determining the effect of flood disturbance on riparian vegetation. The magnitude and frequency of geomorphic processes are reflected in the presence and character of riparian vegetation, which is exemplified in the intermediate-disturbance hypothesis that suggests greater ecological diversity in settings subject to moderate-intensity disturbance (Petraitis and others, 1989).

- Further investigation of the effectiveness of flow management strategies to achieve specific ecological objectives could be achieved through field experiments conducted during managed flow releases (Konrad and others, 2011). Monitoring of physical processes and biological responses during managed reservoir releases, along with predictive modeling, would be useful for quantifying linkages between physical processes and biological responses and for developing recommendations for the timing, duration, and ramping rates for reservoir releases to investigate the minimum flow release required to maximize ecological benefits.

- At locations where fish disease is prevalent, additional ADCP discharge measurements, tracer stones (Papangelakis and others, 2019), or buried accelerometers (Gendaszek and others, 2017), would be useful for constraining the spatial and temporal variability of mobile bed conditions and to validate substrate movement states for larger magnitude armor-disturbing flows.

- As suggested by Alexander and others (2016), three-dimensional hydraulic models, which include the physics of turbulent flow, would be useful for modeling the physical processes that influence polychaete habitat and spore dispersal dynamics at the micro-habitat scale.

Summary and Conclusions

This study used a combination of field and remote sensing methods to assess sediment mobility, river corridor conditions, and river response to flood disturbance. Flood disturbance, during the study period from 2005 to 2019, was produced by a combination of natural flows and reservoir releases and resulted in mobile bed conditions. Direct and indirect evidence is presented, before and after implementation of court-mandated channel-maintenance flows in 2017. Evidence of mobile bed conditions, surface flushing, and episodic scour and fill validate channel-maintenance flow targets defined by Shea and others (2016).

- Sediment transport at (or near) the bed occurred at flows greater than or equal to 5,200 cubic feet per second (ft³/s) at the Iron Gate gage and greater than or equal to 7,700 ft³/s at the Seiad Valley gage.

- The 2006 scour event, with a recurrence interval of greater than or equal to 5–10 years, stripped vegetation from bars and floodplains and caused about 1.0 foot (ft) of degradation at the Seiad Valley gage. Subsequent peak flows, with recurrence intervals of 2–5 years, produced synchronous but transient changes in mean bed elevations from 2007 to 2019 at the two study gages, which are located at the top and bottom of the study reach. Scour during wetter years was followed by fill during intervening dry years, which produced no trend in mean bed elevations.

- The 2017 deep-flushing flow, with a peak flow magnitude of 10,400 ft³/s at the Iron Gate gage and 43,000 ft³/s at the Seiad Valley gage, effectively flushed fine sediment from the surface of low elevation bars at the two ungaged sites.

- Sediment storage in low and high elevation bars increased downstream from Beaver Creek (RKM 48), which indicated a transition from supply limited to equilibrium or transport-limited conditions.

This study evaluated the effectiveness of natural and managed flows for improving river conditions for endangered salmonid populations. In the reach immediately downstream from Iron Gate Dam, substrate disturbance is currently produced during wet years by a combination of natural flows and reservoir releases. During dry years, substrate disturbance relies solely upon reservoir releases.

During the study period from 2005 to 2019, flows greater than 5,200 ft³/s at the Iron Gate gage and greater than 7,700 ft³/s at the Seiad Valley gage initiated sediment transport. Peak flows greater than 6,030 ft³/s initiated localized scour and flushed fine sediment from the channel bed. Peak flows greater than 10,400 ft³/s mobilized coarser bed material, produced deeper scour, and stripped vegetation from bars and floodplains. During the study period, channel maintenance flows released from Iron Gate Dam mobilized, scoured, and disturbed the substrate. Multi-year periods without natural flood disturbance could require periodic flow releases to mobilize sediment and mitigate conditions conducive to *C. shasta*.

References Cited

Alexander, J.D., Bartholomew, J.L., Wright, K.A., Som, N.A., and Hetrick, N.J., 2016, Integrating models to predict distribution of the invertebrate host of myxosporean parasites: Freshwater Science, v. 35, no. 4, p. 1263–1275, https://doi.org/10.1086/688342.

Arthington, A.H., Bunn, S.E., Poff, N.L., and Naiman, R.J., 2006, The challenge of providing environmental flow rules to sustain river ecosystems: Ecological Applications, v. 16, no. 4, p. 1311–1318, https://doi.org/10.1890/1051-0761(2006)016[1311:TCOPEF]2.0.CO;2.

Ayres and Associates, 1999, Geomorphic and sediment evaluation of the Klamath River below Iron Gate Dam: Prepared for the U.S. Fish and Wildlife Service, Yreka, Calif., Cooperative Agreement #14-48-0001-96XXX.

Bartholomew, J.L., Whipple, M.J., Stevens, D.G., and Fryer, J.L., 1997, The life cycle of *Ceratomyxa shasta*, a myxosporean parasite of salmonids, requires a freshwater polychaete as an alternate host: The Journal of Parasitology, v. 83, no. 5, p. 859–868, https://doi.org/10.2307/3284281.

Bendix, J., 1997, Flood disturbance and the distribution of riparian species diversity: Geographical Review, v. 87, no. 4, p. 468–483, https://doi.org/10.2307/215226.

Bunte, K., and Abt, S.R., 2001, Sampling surface and subsurface particle-size distributions in wadable gravel- and cobble-bed streams for analyses in sediment transport, hydraulics, and streambed monitoring: Fort Collins, Colo., U.S. Department of Agriculture, Forest Service, Rocky Mountain Research Station, General Technical Report RMRS-GTR-74, 428 p., https://www.fs.fed.us/rm/pubs/rmrs_gtr074.pdf.

Bureau of Reclamation, 2011, Hydrology, hydraulics, and sediment transport studies for the Secretary's determination on Klamath River Dam removal and basin restoration: Denver, Colo., Bureau of Reclamation, Technical Service Center, Technical Report No. SRH-2011-02, variously paged, https://kbifrm.psmfc.org/file/hydrology-hydraulics-and-sediment-transport-studies-for-the-secretarys-determination-on-klamath-river-dam-removal-and-basin-restoration/.

Carlson, T.N., and Ripley, D.A., 1997, On the relation between NDVI, fractional vegetation cover, and leaf area index: Remote Sensing of Environment, v. 62, no. 3, p. 241–252, https://doi.org/10.1016/S0034-4257(97)00104-1.

Curtis, J.A., and Bond, S., 2020, Sediment mobility and river corridor assessment for a 140-km segment of the mainstem Klamath River below Iron Gate Dam, CA – database of geomorphic features 2010: U.S. Geological Survey data release, https://doi.org/10.5066/P91X3RSF.

Curtis, J.A., and Guerrero, T.M., 2015, Geomorphic mapping to support river restoration on the Trinity River downstream from Lewiston Dam, California, 1980–2011: U.S. Geological Survey Open-File Report 2015–1047, 15 p., https://doi.org/10.3133/ofr20151047.

Curtis, J.A., Wright, S.A., Minear, J.T., and Flint, L.E., 2015, Assessing geomorphic change along the Trinity River downstream from Lewiston Dam, California, 1980–2011: U.S. Geological Survey Scientific Investigations Report 2015–5046, 69 p., https://doi.org/10.3133/sir20155046.

Department of the Interior, Department of Commerce, and National Marine Fisheries Service, 2012, Klamath Dam removal overview report for the Secretary of the Interior–An assessment of science and technical information (version 1.1): U.S. Fish and Wildlife Service, October 2012, https://www.fws.gov/arcata/fisheries/reports/technical/Full%20SDOR%20accessible%20022216.pdf.

Dietrich, W.E., Kirchner, J.W., Ikeda, H., and Iseya, F., 1989, Sediment supply and the development of the coarse surface layer in gravel-bedded rivers: Nature, v. 340, no. 6230, p. 215–217, https://doi.org/10.1038/340215a0.

Fitzpatrick, F.A., Waite, I.R., D'Arconte, P.J., Meador, M.R., Maupin, M.A., and Gurtz, M.E., 1998, Revised methods for characterizing stream habitat in the National Water-Quality Assessment Program: U.S. Geological Survey Water-Resources Investigations Report 98–4052, 67 p., https://doi.org/10.3133/wri984052.

Foott, J.S., Bartholomew, R.J.L., Perry, R.W., and Walker, C.E., 2011, Conceptual model for disease effects in the Klamath River: Whitepaper prepared for the Klamath Basin Restoration Agreement Secretarial Overview Report Process, 12 p., https://kbifrm.psmfc.org/wp-content/uploads/2017/01/Foott-et-al_2011_0063_Conceptual-Model-for-Disease-Effects.pdf.

Gendaszek, A.S., Burton, K., Magirl, C.S., and Konrad, C.P., 2017, Streambed scour of salmon spawning habitat in a regulated river influenced by management of peak discharge: Freshwater Biology, v. 63, no. 8, p. 917–927, https://doi.org/10.1111/fwb.12987.

Hardy, T., and Addley, R.C., 2001, Evaluation of interim instream flow needs in the Klamath River, phase II—Final report to the U.S. Fish and Wildlife Service: Logan, Utah, Utah State University Institute for Natural Systems Engineering, Utah Water Research Laboratory, Utah State University, https://www.fws.gov/yreka/HydroDocs/HardyandAddley2001.pdf.

Holmquist-Johnson, C.L., and Milhous, R.T., 2010, Channel maintenance and flushing flows for the Klamath River below Iron Gate Dam, California: U.S. Geological Survey Open-File Report 2010–1086, 31 p., https://doi.org/10.3133/ofr20101086.

Juracek, K.E., and Fitzpatrick, F.A., 2009, Geomorphic applications of stream-gage information: River Research and Applications, v. 25, no. 3, p. 329–347, https://doi.org/10.1002/rra.1163.

Konrad, C.P., Olden, J.D., Lytle, D.A., Melis, T.S., Schmidt, J.C., Bray, E.N., Freeman, M.C., Gido, K.B., Hemphill, N.P., Kennard, M.J., McMullen, L.E., Mims, M.C., Pyron, M., Robinson, C.T., and Williams, J.G., 2011, Large-scale flow experiments for managing river systems: BioScience, v. 61, no. 1, p. 948–959, https://doi.org/10.1525/bio.2011.61.12.5.

Kondolf, G.M., and Wilcock, P.R., 1996, The flushing flow problem—Defining and evaluating objectives: Water Resources Research, v. 32, no. 8, p. 2589–2599, https://doi.org/10.1029/96WR00898.

Liaw, A., and Wiener, M., 2002, Classification and regression by random forest: R News, v. 2, no. 3, p. 18–22, https://www.r-project.org/doc/Rnews/Rnews_2002-3.pdf.

Lisle, T.E., Nelson, J.M., Pitlick, J., Madej, M.A., and Barkett, B.L., 2000, Variability of bed mobility in natural, gravel-bed channels and adjustments to sediment load at local and reach scales: Water Resources Research, v. 36, no. 12, p. 3743–3755, https://doi.org/10.1029/2000WR900238.

Lund, J., Medellin-Azuara, J., Durand, J., and Stone, K., 2018, Lessons from California's 2012–2016 drought: Journal of Water Resources Planning and Management, v. 144, no. 10, 13 p., https://doi.org/10.1061/(ASCE)WR.1943-5452.0000984.

Malakauskas, D.M., Willson, S.J., Wilzbach, M.A., and Som, N.A., 2013, Flow variations and substrate type affect dislodgement of the freshwater polychaete, *Manayunkia speciosa*: Freshwater Science, v. 32, no. 3, p. 862–873, https://doi.org/10.1899/12-140.1.

McFeeters, S.K., 1996, The use of the normalized difference water index (NDWI) in the delineation of open water features: International Journal of Remote Sensing, v. 17, no. 7, p. 1425–1432, https://doi.org/10.1080/01431169608948714.

Mueller, D.S., 2016, QRev—Software for computation and quality assurance of acoustic doppler current profiler moving-boat streamflow measurements—Technical manual for version 2.8: U.S. Geological Survey Open-File Report 2016–1068, 79 p., https://doi.org/10.3133/ofr20161068.

National Marine Fisheries Service and U.S. Fish and Wildlife Service, 2013, Biological opinions on the effects of proposed Klamath project operations from May 31, 2013, through March 31, 2023, on five federally listed threatened and endangered species: U.S. Fish and Wildlife Service, 590 p., https://www.fws.gov/klamathfallsfwo/news/2013%20BO/2013-Final-Klamath-Project-BO.pdf.

National Research Council, 2004, Endangered and threatened fishes in the Klamath River Basin—Causes of decline and strategies for recovery: Washington, DC, The National Academies Press, https://doi.org/10.17226/10838.

PacifiCorp, 2004, Klamath hydroelectric project study plans, analysis of project effects on sediment transport and river geomorphology: Portland, Oregon, PacifiCorp, 48 p.

Papangelakis, E., Muirhead, C., Schneider, A., and MacVicar, B., 2019, Synthetic radio frequency identification tracer stones with weighted inner ball for burial depth estimation: Journal of Hydraulic Engineering, v. 145, no. 12, 6 p., https://doi.org/10.1061/(ASCE)HY.1943-7900.0001650.

Perry, R.W., Plumb, J.M., Jones, E.C., Som, N.A., Hardy, T.B., and Hetrick, N.J., 2019, Application of the stream salmonid simulator (S3) to Klamath River fall Chinook salmon (*Oncorhynchus tshawytscha*), California—Parameterization and calibration: U.S. Geological Survey Open-File Report 2019–1107, 89 p., https://doi.org/10.3133/ofr20191107.

Petraitis, P.S., Latham, R.E., and Niesenbaum, R.A., 1989, The maintenance of species diversity by disturbance: The Quarterly Review of Biology, v. 64, no. 4, p. 393–418, https://doi.org/10.1086/416457.

Poff, N.L., Allan, J.D., Bain, M.B., Karr, J.R., Prestegaard, K.L., Richter, B.D., Sparks, R.E., and Stromberg, J.C., 1997, The natural flow regime—A paradigm for river conservation and restoration: Bioscience, v. 47, no. 11, p. 769–784, https://doi.org/10.2307/1313099.

Poitras, T.B., and Byrd, K.K, Curtis, J.A., and Bond, S., 2020, Sediment mobility and river corridor assessment for a 140-km segment of the mainstem Klamath River below Iron Gate Dam, CA – vegetation mapping 2005, 2009, 2016: U.S. Geological Survey data release, https://doi.org/10.5066/P9Q2FZK2.

Puckridge, J.T., Sheldon, F., Walker, K.F., and Boulton, A.J., 1998, Flow variability and the ecology of large rivers: Marine and Freshwater Research, v. 49, no. 1, p. 55–72, https://doi.org/10.1071/MF94161.

Rennie, C.D., Vericat, D., Williams, R.D., Brasington, J., and Hicks, M., 2017, Calibration of acoustic doppler current profiler apparent bedload velocity to bedload transport rate, chap 8 *in* Tsutsumi, Daizo, and Laronne, J.B., eds., Gravel-bed rivers—Processes and disasters: John Wiley & Sons Ltd., p. 209–233, https://doi.org/10.1002/9781118971437.ch8.

Schmidt, L.J., and Potyondy, J.P., 2004, Quantifying channel maintenance instream flows—An approach for gravel-bed streams in the Western United States: Fort Collins, Colo., U.S. Department of Agriculture, Forest Service, Rocky Mountain Research Station, General Technical Report RMRSGTR-128, 33 p., https://www.fs.fed.us/rm/pubs/rmrs_gtr128.pdf.

Schmidt, J.C., and Wilcock, P.R., 2008, Metrics for assessing the downstream effects of dams: Water Resources Research, v. 44, no. 4., https://doi.org/10.1029/2006WR005092.

Shea, C., Hetrick, N.J., and Som, N.A., 2016, Response to request for technical assistance—Sediment mobilization and flow history in Klamath River below Iron Gate Dam: Arcata, Calif., U.S. Fish and Wildlife Service Technical Memo, September 29, 2016, https://www.fws.gov/arcata/fisheries/reports/technical/Maintenance%20Flow%20Tech%20Memo%20Final.pdf.

Smelser, M.G., and Schmidt, J.C., 1998, An assessment methodology for determining historical changes in mountain streams: Fort Collins, Colo., U.S. Department of Agriculture, U.S. Forest Service, General Technical Report RMRS-GTR-6, 29 p., https://doi.org/10.2737/RMRS-GTR-6.

Som, N.A., and Hetrick, N.J., 2016, Response to request for technical assistance—*Ceratonova shasta* waterborne spore stages: Arcata, Calif., U.S. Fish and Wildlife Service, Technical Memorandum, https://www.fws.gov/arcata/fisheries/reports/technical/Spores%20Tech%20Memo%20Final.pdf.

Som, N.A., Hetrick, N.J., and Alexander, J.D., 2016a, Response to request for technical assistance—Polychaete distribution and infections: Arcata, Calif., U.S. Fish and Wildlife Service, Technical Memorandum, https://www.fws.gov/arcata/fisheries/reports/technical/Polychaete%20Tech%20Memo%20Final.pdf.

Som, N.A., Hetrick, N.J., Foott, S., and True, K., 2016b, Response to request for technical assistance—Prevalence of *C. shasta* infections in juvenile and adult Salmonids: Arcata, Calif., U.S. Fish and Wildlife Service, Technical Memorandum, https://www.fws.gov/arcata/fisheries/reports/technical/Fish%20Infection%20Tech%20Memo%20AFWO%20Final.pdf.

Stocking, R.W., and Bartholomew, J.L., 2007, Distribution and habitat characteristics of *Manayunkia speciosa* and infection prevalence with the parasite *Ceratomyxa shasta* in the Klamath River, Oregon–California: The Journal of Parasitology, v. 93, no. 1, p. 78–88, https://doi.org/10.1645/GE-939R.1.

Thorsteinson, L., VanderKooi, S., and Duffy, W., eds., 2011, Proceedings of the Klamath Basin science conference, Medford, Oregon, February 1–5, 2010: U.S. Geological Survey Open-File Report 2011–1196, https://doi.org/10.3133/ofr20111196.

Tucker, C.J., 1979, Red and photographic infrared linear combinations for monitoring vegetation: Remote Sensing of Environment, v. 8, no. 2, p. 127–150, https://doi.org/10.1016/0034-4257(79)90013-0.

Turnipseed, D.P., and Sauer, V.B., 2010, Discharge measurements at gaging stations: U.S. Geological Survey Techniques and Methods book 3, chap. A8, 87 p., https://doi.org/10.3133/tm3A8.

U.S. Geological Survey, 2020, National Water Information System: U.S. Geological Survey web interface, https://doi.org/10.5066/F7P55KJN.

Whiting, P.J., 2002, Streamflow necessary for environmental maintenance: Annual Review of Earth and Planetary Sciences, v. 30, no. 1, p. 181–206, https://doi.org/10.1146/annurev.earth.30.083001.161748.

Wilcock, P.R., Kondolf, G.M., Matthews, W.G., and Barta, A.F., 1996, Specification of sediment maintenance flows for a large gravel-bed river: Water Resources Research, v. 32, no. 9, p. 2911–2921, https://doi.org/10.1029/96WR01627.

Wilcock, P., Pitlick, J., and Cui, Y., 2009, Sediment transport primer—Estimating bed-material transport in gravel-bed rivers: Fort Collins, Colo., General Technical Report RMRS-GTR-226, U.S. Department of Agriculture, Forest Service, Rocky Mountain Research Station, 78 p., https://www.fs.fed.us/rm/pubs/rmrs_gtr226.pdf.

Wohl, E., Bledsoe, B.P., Jacobson, R.B., Poff, N.L., Rathburn, S.L., Walters, D.M., and Wilcox, A.C., 2015, The natural sediment regime in rivers—Broadening the foundation for ecosystem management: Bioscience, v. 65, no. 4, p. 358–371, https://doi.org/10.1093/biosci/biv002.

Woolpert, Inc., 2010, LiDAR report— Klamath River LiDAR and mapping, 2010—Link River Dam, Oreg., to the confluence with Elk Creek south of Happy Camp, CA: U.S. Bureau of Reclamation Contract No: 08-CA-40-8258, Task Order: R10PD40007, https://www.oregongeology.org/pubs/ldq/reports/Klamath_River_2010_Lidar_Report.pdf.

Wright, K.A., Goodman, D.H., Som, N.A., and Hardy, T.B., 2014, Development of two dimensional hydraulic models to predict distribution of Manayunkia speciosa in the Klamath River: Arcata, Calif., U.S. Fish and Wildlife Service, Arcata Fish and Wildlife Office, Arcata Fisheries Technical Report Number TR 2014-19, https://pdfs.semanticscholar.org/c67c/b68880297eab06d8658400d56641a986c5d7.pdf?_ga=2.74970327.419090957.1592588807-1673815459.1592588807.

Yu, Q., Gong, P., Clinton, N., Biging, G., Kelly, M., and Schirokauer, D., 2006, Object-based detailed vegetation classification with airborne high spatial resolution remote sensing imagery: Photogrammetric Engineering and Remote Sensing, v. 72, no. 7, p. 799–811, https://doi.org/10.14358/PERS.72.7.799.

Appendix 1.

XML files for each discharge measurement listed in table 1.1 and 1.2 are available at https://doi.org/10.3133/ofr20201141.

USGS